JGR Atmospheres

RESEARCH ARTICLE
10.1029/2023JD039902

Trends in Seasonal Mean Speciated Aerosol Composition in Remote Areas of the United States From 2000 Through 2021

J. L. Hand[1], **A. J. Prenni**[2], **and B. A. Schichtel**[2]

[1]Cooperative Institute for Research in the Atmosphere, Colorado State University, Fort Collins, CO, USA, [2]National Park Service, Air Resources Division, Lakewood, CO, USA

Key Points:

- Fine mass seasonal mean concentrations have significantly decreased in remote regions of the U.S. in response to regulatory activity
- Sulfate aerosols have decreased at the highest rate, followed by nitrate, elemental carbon, fine dust, and organic carbon
- Flat and insignificant trends in organic carbon and fine mass at western sites in summer/fall were influenced by biomass smoke emissions

Supporting Information:

Supporting Information may be found in the online version of this article.

Correspondence to:

J. L. Hand,
jlhand@colostate.edu

Citation:

Hand, J. L., Prenni, A. J., & Schichtel, B. A. (2024). Trends in seasonal mean speciated aerosol composition in remote areas of the United States from 2000 through 2021. *Journal of Geophysical Research: Atmospheres*, *129*, e2023JD039902. https://doi.org/10.1029/2023JD039902

Received 29 AUG 2023
Accepted 23 DEC 2023

Author Contributions:

Conceptualization: J. L. Hand, A. J. Prenni, B. A. Schichtel
Formal analysis: J. L. Hand
Methodology: J. L. Hand, A. J. Prenni, B. A. Schichtel
Visualization: J. L. Hand
Writing – original draft: J. L. Hand
Writing – review & editing: A. J. Prenni, B. A. Schichtel

Abstract Large reductions in anthropogenic emissions of particulate matter and its precursor emissions have occurred since the enactment of the Clean Air Act Amendments of 1990. The Interagency Monitoring of Protected Visual Environments network has measured $PM_{2.5}$ gravimetric mass (mass of particles with aerodynamic diameters less than 2.5 μm, also referred to here as fine mass, "FM") and speciated $PM_{2.5}$ aerosol composition at remote sites since 1988. Measured species include inorganic anions such as sulfate, nitrate, and chloride, carbonaceous aerosols such as organic (OC) and elemental carbon (EC), and elemental concentrations used to estimate fine dust (FD). Trends in seasonal and annual mean mass concentrations were calculated from 2000 through 2021, a period that includes the largest reductions in emissions. On average, annual mean FM at remote sites in the continental United States has decreased at a rate of −1.8% yr^{-1}. This reduction is largely due to annual mean trends in sulfate (−6.1% yr^{-1}), nitrate (−2.7% yr^{-1}), EC (−2.2% yr^{-1}), FD (−1.3% yr^{-1}), and OC (−0.9% yr^{-1}), although the OC annual mean trend was insignificant. Seasonal and regional mean FM trends varied significantly, with strong reductions in the East in all seasons due to sulfate reductions, and flat and insignificant trends in summer and fall in the West due to the influence of biomass burning emissions on OC trends. Evaluating regional and seasonal mean trends in aerosol composition helps identify sources that continue to adversely impact air quality and hinder progress in FM reductions due to successful regulatory activity.

Plain Language Summary Particulate matter in the atmosphere is made up of many species that have both anthropogenic and natural sources. Thanks to the Clean Air Act Amendments of 1990, anthropogenic emissions that lead to some particulate matter (PM) have decreased, which has resulted in measurable improvements in air quality in remote regions of the United States. Evaluating trends in aerosol measurements from a large-scale monitoring network over the past two decades has shown that at remote sites in the United States, some aerosol species, like sulfates, nitrates, and some carbonaceous aerosols, have decreased significantly due to the emission reductions; but others, like mineral dust and carbonaceous aerosols from wildfire smoke, have not. In order to continue to make progress in improving air quality in the United States, targeting future sources for emission reductions will require accurate assessments of the contributions from these sources. Dust and wildfire smoke contributions to PM in remote locations across the United States are now larger fractions compared to two decades ago and will likely continue to grow with climate change.

1. Introduction

The major constituents of $PM_{2.5}$ (particles with aerodynamic diameters less than 2.5 μm, referred to here as fine mass, "FM") in the remote and rural United States include inorganic species such as sulfate and nitrate, carbonaceous aerosols such as organic matter and elemental carbon (EC), fine mineral dust aerosols (FD), and sea salt. These species have different sources, lifetimes, and seasonality, and influence air quality on local to global scales. They also have different and wide-ranging impacts on visibility (e.g., Hand et al., 2020), climate (e.g., Samset et al., 2018), health (e.g., Shiraiwa et al., 2017), cloud processes (e.g., Seinfeld et al., 2016), and ecology (e.g., Field et al., 2010), among others. These impacts are more accurately estimated when FM and its contributing species are measured concurrently.

Sulfate is a major contributor to FM in the United States and the majority of sulfate in the atmosphere is produced through chemical reactions of sulfur dioxide (SO_2). Anthropogenic SO_2 is emitted through industrial activities including coal and diesel fuel combustion. Regions that host electric utilities and industrial boilers (e.g., the eastern United States) tend to have the highest SO_2 emissions. Oxidation of SO_2 to particulate sulfate occurs

through homogeneous and heterogeneous reactions, with aqueous chemistry being the most efficient. The degree of acidity of sulfate (from acidic sulfuric acid to fully neutralized ammonium sulfate) depends on the environmental conditions and availability of ammonia. Sulfate acidity varies spatially and temporally, with recent studies showing that in the East, sulfate is in a more acidic form than in the West (Chen et al., 2019; Hidy et al., 2014; Kim et al., 2015; Lawal et al., 2018; Lowenthal et al., 2015; Silvern et al., 2017; Weber et al., 2016).

Fine particulate nitrate, often in the form of ammonium nitrate, is created from the reversible reaction of gas-phase ammonia and nitric acid. Sources of oxidized nitrogen include combustion of fossil fuels from point sources, including coal-fired powered plants and mobile sources. Other important sources of oxidized nitrogen include biomass burning, lightning, and biogenic sources in soil (Vitousek et al., 1997). Ammonia is primarily emitted from agricultural activities, but mobile sources and natural emissions can also be significant contributors. Lower temperatures and higher relative humidity favor particulate ammonium nitrate formation. The central United States is an area of high agricultural activity and is associated with high nitrate and ammonium concentrations that can lead to elevated fine-mode ammonium nitrate concentrations (Heald et al., 2012; Hu et al., 2020; Pitchford et al., 2009; Warner et al., 2017).

The sources of organic carbon (OC) in the atmosphere are both primary emissions and secondary formation. Primary emissions include particle mass emitted directly from combustion of fossil fuels or biomass. Secondary organic aerosol formation results from the oxidation of gas-phase precursors (volatile organic carbons, VOCs) from both anthropogenic and biogenic sources. Elemental carbon (EC), also referred to as light absorbing carbon or black carbon (BC) depending on the measurement method (Petzold et al., 2013), is emitted directly from incomplete combustion of fossil fuels or biomass (e.g., Bond et al., 2013).

Sources of mineral dust in the atmosphere include both natural and anthropogenic sources, including entrainment from deserts, paved and unpaved roads, agricultural activity, construction, and fire. The seasonal and spatial variability of dust in the United States is influenced by both local, regional, and long-range transport. Several studies have shown that contributions of Asian dust to U.S. fine dust concentrations can be significant episodically, affecting aerosol concentrations and mineralogy across the United States, typically in the spring (e.g., Creamean et al., 2014; Hand et al., 2017; Husar et al., 2001; Kim et al., 2021; Prospero et al., 2002). Transport of North African dust to the United States occurs regularly in summer, affecting aerosol concentrations in the Virgin Islands and the eastern and southeastern United States (Aldhaif et al., 2020; Bozlaker et al., 2019; Hand et al., 2017; Perry et al., 1997; Prospero et al., 2021). Dust concentrations in desert regions of the Southwest arise from local and regional sources as well as transboundary transport from the Chihuahuan desert in Mexico, especially in winter and spring (Hand et al., 2016, 2017; Rivera et al., 2009; Tong et al., 2012). Dust in the central United States is influenced by agricultural activity (Hand et al., 2017; Lambert et al., 2020; Pu & Ginoux, 2018).

Sea salt can be a significant fraction of FM in many coastal locations, as well as contribute significantly to light scattering (e.g., Lowenthal & Kumar, 2006; Murphy et al., 2019). Sea salt concentrations are typically computed from sea salt markers like sodium ion, chloride ion, or a combination of ions. Sea salt may be underestimated when using the chloride ion or chlorine to estimate sea salt, due to depletion of chloride from the reaction of gaseous nitric acid with sea salt that produces sodium nitrate particles and the release of gaseous hydrochloric acid (White, 2008).

Many earlier studies have demonstrated that aerosol composition in the United States has changed in response to the enactment of the Clean Air Act Amendments of 1990 that regulated emissions of gaseous precursors such as SO_2 and nitrogen oxides (NO_x). These reductions led to decreases in secondary aerosols such as sulfate and nitrate concentrations and deposition (Attwood et al., 2014; Beachley et al., 2016; Benish et al., 2022; Blanchard et al., 2013; Du et al., 2014; Ellis et al., 2013; Feng et al., 2020; Hand, Schichtel, et al., 2012; Lawal et al., 2018; Lehmann & Gay, 2011; Malm et al., 2002; Nopmongcol et al., 2019; Sickles & Shadwick, 2015; Zhang et al., 2018). OC concentrations in the eastern United States have declined due to reductions in emissions (Blanchard et al., 2016; Malm et al., 2017; Ridley et al., 2018). However, biomass smoke emissions have been shown to influence trends in high concentrations of OC and FM (McClure & Jaffe, 2018). Trends in FD are influenced by large-scale climate variability (Hand et al., 2016; Pu & Ginoux, 2018), and local and regional drought conditions (e.g., Achakulwisut et al., 2019), as well as land-use change (Lambert et al., 2020).

Modeling studies have also demonstrated the impacts of reduced emissions on aerosol concentrations and radiative properties. For example, Leibensperger et al. (2012) demonstrated that aerosol forcing decreased sharply

from 1990 through 2010 due mainly to SO_2 emission reductions. Changes in SO_2 and NO_x emissions from 1995 through 2010 also lead to changes in aerosol shortwave radiative forcing, in particular demonstrating a connection between shortwave radiation "brightening" and aerosol loading, especially in the eastern United States (Gan et al., 2015). Simulations of air quality from 1990 through 2010 using the Community Multiscale Air Quality model were also able to reproduce observed trends in the United States, especially for SO_2, nitrogen dioxide, and EC (Xing et al., 2015). However, the model failed to capture trends in nitrate, potentially due to uncertainties in ammonia emissions.

FM trend analysis quantifies the changes in FM concentrations over time, but linking changes in FM to source emissions requires understanding changes in speciated composition. Because speciated aerosols have different sources, with varying seasonal, local, and regional impacts, analyzing seasonal mean trends is important for understanding how changes in emission sources impact air quality. Data from long-term monitoring networks are crucial for evaluating changing concentrations and identifying their relationships to emission sources. Speciated aerosol data from remote and rural sites in the Interagency Monitoring for Protected Visual Environments (IMPROVE) network were used to evaluate trends of seasonal and annual mean concentrations in FM, sulfate, nitrate, OC, EC, and FD from 2000 through 2021. The spatial and seasonal variability in speciated trends were compared to emission sources to identify the influence of different sources. Identifying impacts from a particular species on FM trends can aid management strategies that target specific sources. The results presented here extend and expand on previous trend studies by investigating the spatial variability in seasonal mean speciated aerosol trends and their impacts on FM. Evaluating seasonal trends helps account for the interannual variability in sources and atmospheric processes on changes in aerosol concentrations.

2. Methods

The IMPROVE network has been operating since 1988 with the main purpose of tracking trends in aerosol composition and haze in remote areas of the United States (Malm et al., 1994). In 2000 the network expanded in support of monitoring for the Environmental Protection Agency's (EPA) Regional Haze Rule. The IMPROVE network currently operates around 155 mostly remote and rural sites across the United States. Aerosol filters are collected for 24 hr (midnight to midnight local standard time) every third day and concentrations are reported at local ambient conditions. Filters are analyzed for inorganic ions using ion chromatography, carbonaceous aerosols using Thermal Optical Reflectance (TOR, Chow et al., 2007), and elemental concentrations using X-Ray fluorescence (XRF). Changes to the network monitoring and analysis have occurred over time; these changes are reported by Hand et al. (2019, 2023) and through data advisories on the IMPROVE website. Additional analysis and monitoring information, including site locations, can be found in Hand et al. (2023). Daily aerosol data from 2000 through 2021 were downloaded for only remote/rural sites from the Federal Land Manager Environmental Database (FED) on 11 April 2023, including FM, sulfate, nitrate, chloride, OC, EC, and elemental species. While sea salt can contribute significantly to particulate matter (PM), especially at coastal sites, it was not considered for trend analysis due to filter blank contamination in the early 2000s that may influence trends (Hand et al., 2019; Zhang, 2019).

Gravimetric mass measurement is an operationally defined analysis and may have sampling or analytical artifacts that can influence FM trends. For example, nitrate loss and volatilization of some organic species contribute to negative artifacts (e.g., Chow et al., 2005, 2010; Hering & Cass, 1999; Watson et al., 2009), while positive artifacts include retention of water associated with hygroscopic species (Frank, 2006; Hand et al., 2019). Beginning in 2011, higher laboratory relative humidity during weighing resulted in an increase in particle bound water associated with FM data (White, 2016). This issue was resolved in 2019, but it may influence trends in FM (Hand et al., 2019). Seasonal variability of species that are associated with FM biases may confound interpretation of seasonal mean trends in FM.

To reduce impacts from missing data on trend results, missing sulfate concentrations were replaced with sulfur concentrations scaled to sulfate mass ($3 \times$ sulfur, Hand, Schichtel, et al., 2012). IMPROVE nitrate ion concentrations at many sites fell below historical values during winter months from 1996 through 2000; the cause remains unknown (McDade, 2004, 2007). Nitrate concentrations returned to normal levels after 2000, after which the data were deemed valid. Given the number of sites influenced by this anomaly (Debell, 2006), nitrate ion data were considered invalid during winter months of 2000.

Trends in OC and EC may be affected by changes in analytical methods. A review of carbonaceous measurements in the IMPROVE program identified shifts in analytical methods and their impacts on the fraction of EC to total carbon (OC + EC), that is, EC/TC (Schichtel et al., 2021). One such shift occurred with hardware upgrades in 2005 that resulted in changes in the split between OC and EC derived from the TOR measurement that introduced uncertainty to trend analyses (Chow et al., 2007; White, 2007). Other shifts in EC/TC have also occurred over the history of the program due to new analyzers, new calibrations, and undetermined reasons. EC trends are also affected by hardware and analytic changes, similar to issues that affect OC trends. In addition, Malm et al. (2020) suggested EC may be inadvertently and incorrectly assigned to the OC fraction during the TOR analysis, resulting in an underestimate of true EC concentrations. As discussed by Schichtel et al. (2021), EC concentrations have decreased at rural sites to the point that many sites have concentrations that are below the lower quantifiable limits (LQL, defined as 3 × minimum detection level (MDL)). From 2017 to 2019, about 30% of all EC concentrations were below the LQL. More sites in the West were below LQL than in the East (Schichtel et al., 2021). These low concentrations can lead to difficulties in tracking trends, especially for very low concentrations.

FD concentrations are estimated by summing the oxides of elements typically associated with soil, with a correction for other compounds such as carbonates (Malm et al., 1994). Elemental concentrations are multiplied by factors that account for mass concentrations of the oxide forms. FD concentrations were increased by 15% to reflect biases identified by Hand et al. (2019) (Equation 1).

$$FD = 1.15 \times (2.2 \times [Al] + 2.49 \times [Si] + 1.63 \times [Ca] + 2.42 \times [Fe] + 1.94 \times [Ti]) \quad (1)$$

The analytical methods used to determine elemental concentrations have evolved over time (Hyslop et al., 2015; Spada et al., 2023). In 2011, the analysis method switched to the PANalytical XRF system that resolved issues related to undetected Al with concentrations above the MDL (White, 2006). Before 2011, XRF data below the MDL were replaced by 0.5 × MDL. Changes in analytical methods may not equally affect data for each FD species; therefore, the integrated FD concentration calculated with Equation 1 may be less susceptible to possible variability introduced by the analytical methods, although this has not been specifically demonstrated.

All species concentrations are reported with adjustments for blank corrections (Hand et al., 2023). With the exception of data derived from XRF, data were used as reported, that is, no substitutions were performed for data below MDLs.

Seasonal mean concentrations were calculated for winter (DJF), spring (MAM), summer (JJA), and fall (SON) from 2000 through 2021. December data from the previous year were included in winter mean calculations. Fifty percent of daily data was required for a valid seasonal mean, and annual means were calculated from four valid seasonal means. Trends required 70% of the valid seasonal and annual means over the time period for data from a site to be included in trend calculations, resulting in around 130 to 140 sites, depending on season and species. Data were also aggregated over a four year period (2018–2021) to evaluate the recent status in speciated concentrations; for annual mean concentrations, roughly 152 sites met the completeness criteria, depending on species.

A Theil regression was performed with the concentration data as the dependent variable and the year as the independent variable. Theil regressions avoid heavy influence by outliers on the regression results (Theil, 1950). Kendall tau statistics were used to determine the statistical significance, assuming the slope was statistically significant at 5% ($p \leq 0.05$), meaning that there was a 95% chance that the slope was not due to random chance. Trends (% yr^{-1}) were calculated by dividing the slope by the median concentration value over the time period of the trend, multiplied by 100%. Reporting trends instead of slopes normalizes the range in concentrations that occur across the United States. However, trends can be large when median concentrations are very low. Site-specific annual mean aggregated concentrations and seasonal mean trend results were interpolated to provide isopleths to guide the eye (Isaaks & Mohan Srivastava, 1989).

Regional mean trends were calculated for 10 regions of the United States. Sites were grouped by their state into the following regions: Northeast, Southeast, Midsouth, Central, Southwest, Northwest, California, Alaska, Hawaii, Virgin Islands (see Table 1) and the continental United States (CONUS). The regions were qualitatively determined based on spatial patterns in FM trends and serve only as a means for summarizing trends. Regional mean trends were computed by aggregating site-specific seasonal mean concentrations for a given region and year and then performing a Theil regression on regional mean concentrations. Sites that met the 70% completeness criterion for a given species and season were included in the regional trend calculation. Regional mean

Table 1
Regions and States (Abbreviations) Used for Regional Mean Trends

Region	State abbreviation
Northeast	ME, NH, VT, MA, RI, CT, NY, PA, NJ, DE, MD, OH, WV, VA, IN, KY
Southeast	TN, NC, SC, MS, LA, AL, GA, FL
Midsouth	OK, LA, AR
Central	ND, SD, MN, MI, WI, IL, MO, KS, NE, IA
Southwest	NV, UT, CO, NM, AZ, TX
Northwest	WA, OR, ID, MT, WY
California	CA
Alaska	AK
Hawaii	HI
Virgin Islands	Virgin Islands

Note. Sites within listed states were included in the corresponding region.

trends were calculated for seasonal and annual means. Periods for regional trends were shortened (2002 through 2021) relative to site-specific trends to limit influences of biases due to sites coming on-line during the early years of network expansion in 2000 (Hand et al., 2014; Schichtel et al., 2011).

The EPA reports an annual National Emission Inventory (NEI) for criteria pollutants such as SO_2, nitrogen oxides (NO_x), VOCs, and BC as a function of source category. Emission data corresponding to all reported categories were downloaded from the NEI database for annual emissions from 1970 through 2022 for the entire United States. Total wildland fire acreages from 1983 through 2021 for the United States were downloaded from the National Interagency Fire Center (NIFC) database. Data from 2004 do not include state lands for North Carolina. The Pacific Decadal Oscillation (PDO) indices were downloaded from the National Centers for Environmental Information (NCEI) database. The NCEI index is based on the National Oceanic and Atmospheric Administration's extended reconstruction of sea surface temperatures. PDO indices for all months from 1854 through 2023 are available. Data for NEI, burn acreage, and PDO indices were downloaded on 18 August 2023.

3. Fine Mass and Speciated Aerosol Concentrations

The 2018 through 2021 annual mean $PM_{2.5}$ speciated mass concentrations are shown in Figures (1a–1f) for sulfate, nitrate, OC, EC, FD, and FM, respectively. For each figure, the contour levels were created with the highest level corresponding to the 95th percentile in annual mean mass concentration for all sites, shown as circles. Isopleths in mass concentration serve to guide the eye for spatial patterns and are not for strict interpretation.

The highest annual mean sulfate ion concentrations in the CONUS occurred at sites around the eastern United States (~1 μg m^{-3}) (see Figure 1a). Sulfate concentrations decreased sharply at sites in the western United States, where concentrations were less than 0.5 μg m^{-3}, with the lowest concentrations at sites in the Northwest and Intermountain West. This spatial gradient in sulfate has existed for decades (e.g., Husar et al., 1981; Malm et al., 1994). Concentrations in the West reflected lower SO_2 emissions that lead to secondary particulate sulfate (Hand, Schichtel, et al., 2012, 2020). Somewhat higher concentrations occurred at sites in southern California, and at sites in the Northern Great Plains. Concentrations in the northwestern United States were less than 0.3 μg m^{-3}, indicating transboundary contributions were lower than previous modeling studies suggest (Park et al., 2004, 2006) possibly due to reduced emissions in Asia (Shi et al., 2022).

The spatial pattern in nitrate differed from sulfate in that the area of high annual mean nitrate concentrations (~0.8 μg m^{-3}) occurred in the central United States (Figure 1b) where intensive agricultural activity occurs (Hu et al., 2020; Pitchford et al., 2009). Sites in central and southern California also had higher annual mean nitrate concentrations. Sites with elevated concentrations in northern North Dakota may be associated with oil and gas energy development (e.g., Prenni et al., 2016). High annual mean concentrations were observed at Dinosaur National Monument in Colorado, also likely associated with oil and gas development (Prenni et al., 2022). Concentrations were much lower at sites in the Intermountain West and Northwest, with annual mean concentrations less than 0.3 μg m^{-3}. Similarly, low annual mean concentrations occurred at sites in the Southeast and Northeast.

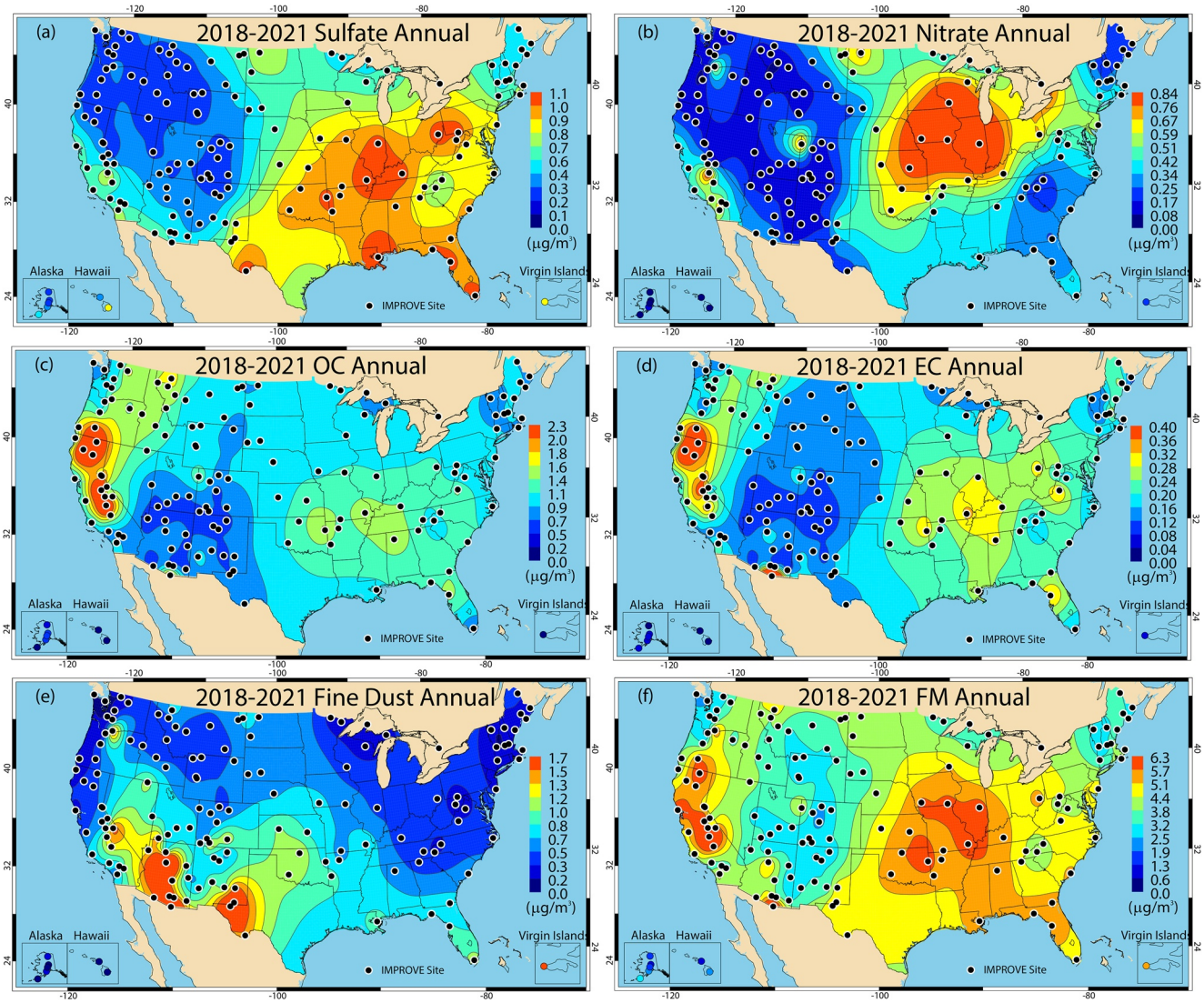

Figure 1. Interagency Monitoring of Protected Visual Environments 2018–2021 annual mean $PM_{2.5}$ concentrations (μg m^{-3}) for (a) sulfate ion, (b) nitrate ion, (c) organic carbon (OC) (d) elemental carbon (EC), (e) fine dust (FD), and (f) gravimetric fine mass (FM).

Unlike spatial patterns in sulfate and nitrate, the highest annual mean OC concentrations (>2 μg m^{-3}) occurred at sites in central and northern California and the northwestern United States due to the influence of biomass burning (Figure 1c). OC concentrations that are highly influenced by biomass burning may be underestimated, since the high concentrations can cause filter clogging and loss of data. Elevated annual mean levels of OC (1–2 μg m^{-3}) also occurred at sites across the eastern United States, likely associated with biogenic and anthropogenic emissions. Blanchard et al. (2016) reported that roughly half of the organic aerosol in the southeastern United States from 1999 to 2003 was attributed to combustion processes, including from fossil fuel and biomass burning. They also identified the importance of biogenic emissions to organic aerosol in the Southeast, as did Schichtel et al. (2017) and Xu et al. (2018). Annual mean concentrations were lowest at sites in the Southwest (<1 μg m^{-3}).

The spatial pattern in annual mean EC concentrations was similar to OC, especially at sites in the western United States where biomass smoke emissions have influenced both species (Figure 1d). Annual mean EC was over 0.4 μg m^{-3} at many of these sites. EC concentrations were also elevated (~0.2–0.3 μg m^{-3}) at sites across the eastern United States, many coinciding with sites that had high OC. Concentrations were relatively low at sites across the Southwest and Intermountain West (<0.2 μg m^{-3}).

Unlike the east-west gradient observed for sulfate, nitrate, OC, and EC, annual mean FD concentrations exhibited a north-south gradient with higher concentrations at sites in the southern United States (Figure 1e). FD concentrations at sites in desert regions of the Southwest are higher due to the impacts of local and regional sources, and FD at sites in the central United States is influenced by agricultural activity. At sites in the Southeast, FD concentrations are influenced by transport of dust from North Africa. The highest annual mean concentrations were observed at sites in the Southwest (>1.5 μg m^{-3}). Concentrations of FD at sites in the northern United States were typically less than 0.5 μg m^{-3}, with the exception of higher FD concentrations near Columbia River Gorge, Washington and at sites in northern Montana and North Dakota.

The spatial pattern of 2018–2021 annual mean FM concentrations at remote sites reflected the combined patterns of sulfate, nitrate, OC, and FD (see Figure 1f). The highest concentrations of annual mean FM (>5 μg m^{-3}) occurred at remote sites in the central and eastern United States, likely due to impacts from sulfate, nitrate, and OC. Similarly, high FM concentrations at sites in the West were likely due to impacts from OC. The lowest FM concentrations occurred at sites in the Intermountain West, where speciated concentrations were relatively low. The highest annual mean FM concentration was 9.7 μg m^{-3} at Sequoia National Park, California, which is below the current annual primary National Ambient Air Quality Standard of 12 μg m^{-3}, but near the new proposed standard of 9–10 μg m^{-3}.

Changes in FM depend on the species that compose it. Timelines of regional, annual mean mass concentrations for FM, ammonium sulfate (AS), ammonium nitrate (AN), particulate organic matter (POM), EC, FD, and sea salt (SS) are shown in Figures 2(a–2j), respectively, for the summary regions defined in Section 2. For only this figure, mass correction factors were applied to individual species in order to represent contributions to total FM. Sulfate was assumed to be fully neutralized ammonium sulfate (AS = 1.375 × sulfate ion) and nitrate was assumed to be ammonium nitrate (AN = 1.29 × nitrate ion). A constant organic carbon multiplier of 1.8 was used for the entire year to calculate particulate organic matter (POM = 1.8 × OC) to avoid obfuscating seasonal OC trends. Sea salt was calculated using chloride ion data (SS = 1.7 × chloride ion). Timelines of regional mean FM are also shown. An investigation into differences in FM and the sum of individual species was reported by Hand et al. (2019).

Species concentrations and contributions to FM varied for each region, and for some regions the contributions have changed over time. For example, AS was a major fraction of FM in the early 2000s, especially in eastern regions such as the Central, Midsouth, Northeast, the Southeast regions (Figures 2f–2i, respectively). AS concentrations have dramatically decreased in these regions and is a lower contributor to FM on an annual mean basis. Over time, POM has grown in its contribution to FM, although its absolute concentration has decreased, especially at regions in the East. In western regions, POM was a major contributor to FM, and its contributions have increased as contributions from other species, such as AS and AN, have decreased. Impacts from high fire years (2017–2018, 2020–2021) were evident in the Northwest and the California regions (Figures 2c and 2d, respectively), and to a lesser degree in the Southwest region (Figure 2e). FD contributions were highest in the Southwest region (Figure 2e), although they were non-negligible at western regions the Northwest and California regions (Figures 2c and 2d, respectively), and even in the Central and Midsouth regions (Figures 2f and 2g, respectively). The contributions from SS are evident at coastal regions. OCONUS (outside the continental United States) regions were each dominated by different species. The Virgin Islands region was dominated by FD, while the Alaska region had very low FD contributions and instead was dominated by AS, POM, and SS. In the Hawaii region, AS is the major contributor to FM, and decreased significantly in 2019, following the eruption of the Kīlauea volcano in Hawaii Volcanoes National Park, and the dramatic decrease in SO_2 concentrations (see Figure S1 in Supporting Information S1). For the total CONUS (Figure 2j), the major contributing species has shifted from AS to POM.

4. Trends

The mass concentration timelines shown in Figure 2 indicate significant changes in speciated composition, as well as FM, over the past two decades. Trend analyses provide a quantitative investigation of the observed changes.

4.1. Gravimetric Fine Mass

The spatial and seasonal variability in FM trends can be understood by examining the trends in others major contributing species. In this section, trends in FM first are presented, followed by trends in the species shown in Figure 1. Individual site trends are shown on maps with isopleths in percent per year. Negative trends are shown with downward-pointing triangles and contoured with cold colors, while positive trends are shown with upward-pointing triangles and warm colors. Trends with p-values less than or equal to 0.05 ($p \leq 0.05$) are

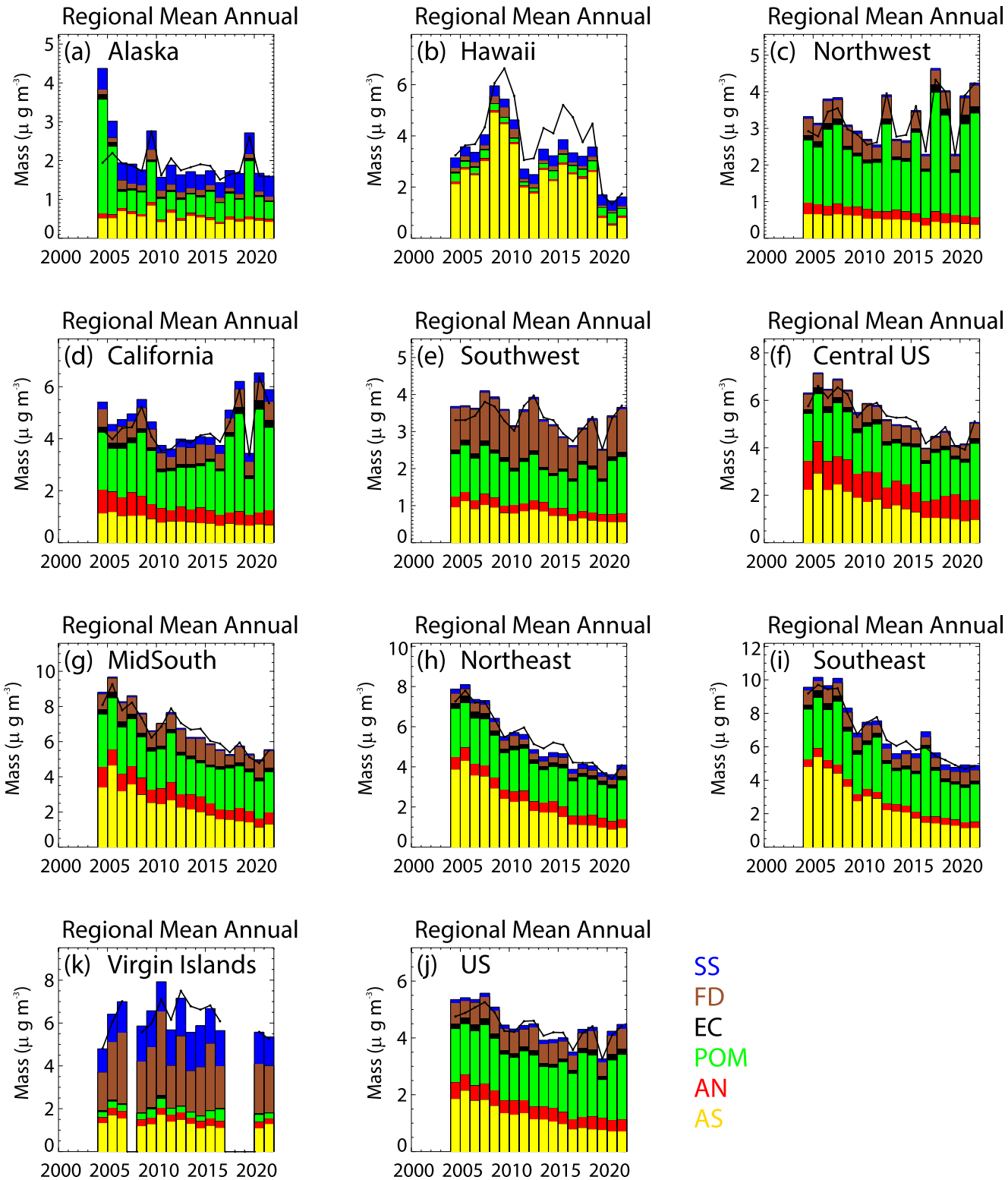

Figure 2. Interagency Monitoring of Protected Visual Environments regional, annual mean mass concentrations (μg m^{-3}) for ammonium sulfate (AS), ammonium nitrate (AN), particulate organic matter (POM), elemental carbon (EC), fine dust (FD), sea salt (SS), and gravimetric fine mass (FM, shown as the black line) for major summary regions.

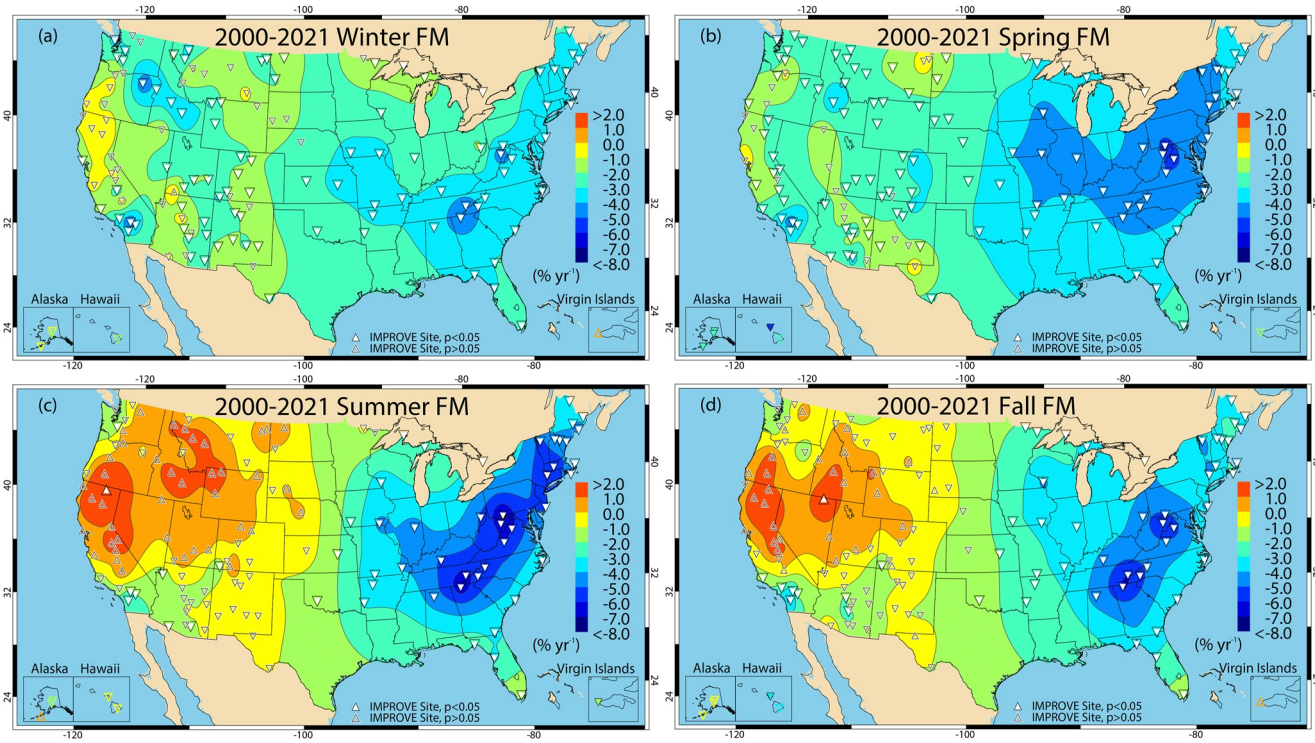

Figure 3. Seasonal mean $PM_{2.5}$ gravimetric fine mass (FM) trends (% yr^{-1}) from 2000 to 2021 for (a) winter (DJF) (b) spring (MAM) (c) summer (JJA), and (d) fall (SON). Filled triangles correspond to statistically significant trends ($p \leq 0.05$).

considered statistically significant and denoted with filled triangles. Scales were kept similar for all parameters so that trends can be compared. Isopleths in regions without sites should be viewed only as a spatial transition.

Seasonal mean trends in FM are shown in Figure 3. The strongest reductions in FM occurred at sites in the eastern United States, especially in summer and fall (Figures 3c and 3d, respectively), with trends around −6% yr^{-1} to −7% yr^{-1}. The strongest reduction of −7.6% yr^{-1} ($p < 0.001$) occurred in summer in Frostburg Reservoir, Maryland (site code, FRRE1) and of −6.3% yr^{-1} ($p < 0.001$) in fall in Cohutta, Georgia (COHU1). Positive trends in summer and fall occurred in summer in Lava Beds, California (4.9% yr^{-1}, $p = 0.040$; LABE1) and in fall in Jarbidge, Nevada (2.4% yr^{-1}, $p = 0.022$; JARB1). These positive trends at sites in the West are part of a larger, regional pattern of sites across the West with positive but insignificant trends during summer and fall. Insignificant trends also occurred at sites in the Northern Great Plains in spring and California and Oregon in winter. The strong spatial gradient in trends at sites between the East and the West during summer and fall indicated sources with regional influence on FM, such as biomass smoke emissions. During winter and spring the spatial gradient weakened, with negative trends across the United States, and the strongest reductions at sites in the East.

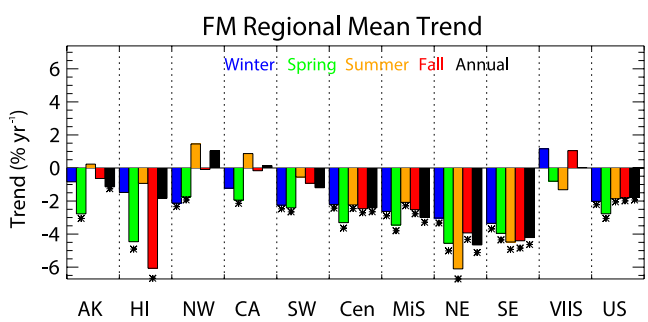

Figure 4. Regional, seasonal mean $PM_{2.5}$ gravimetric fine mass (FM) trends (% yr^{-1}) from 2002 to 2021 for major U.S. regions for winter, spring, summer, fall, and annual means. Regions are arranged from west to east (AK = Alaska, HI = Hawaii, NW = Northwest, CA = California, SW = Southwest, Cen = Central, MiS = Midsouth, NE = Northeast, SE = Southeast, VIIS = Virgin Islands, and U.S. = all continental sites). Statistically significant trends ($p \leq 0.05$) are denoted with "*".

Statistically significant regional, seasonal mean trends in FM were negative across most U.S. regions (Figure 4). The strongest reductions in FM occurred in the Northeast and Southeast regions during summer (−4% yr^{-1} to −5% yr^{-1}) and the weakest seasonal trends occurred in winter (~−3% yr^{-1}). Trends in the Midsouth and Central regions were less negative than in eastern regions, with the strongest trends in spring (~−3% yr^{-1}). FM decreased significantly during spring and winter at regions in the West; however, summer and fall trends were flat and insignificant, reflecting the spatial patterns seen in Figure 3. The overall annual mean trend for the United States was −1.8% yr^{-1} ($p < 0.001$). Timelines for seasonal, regional mean

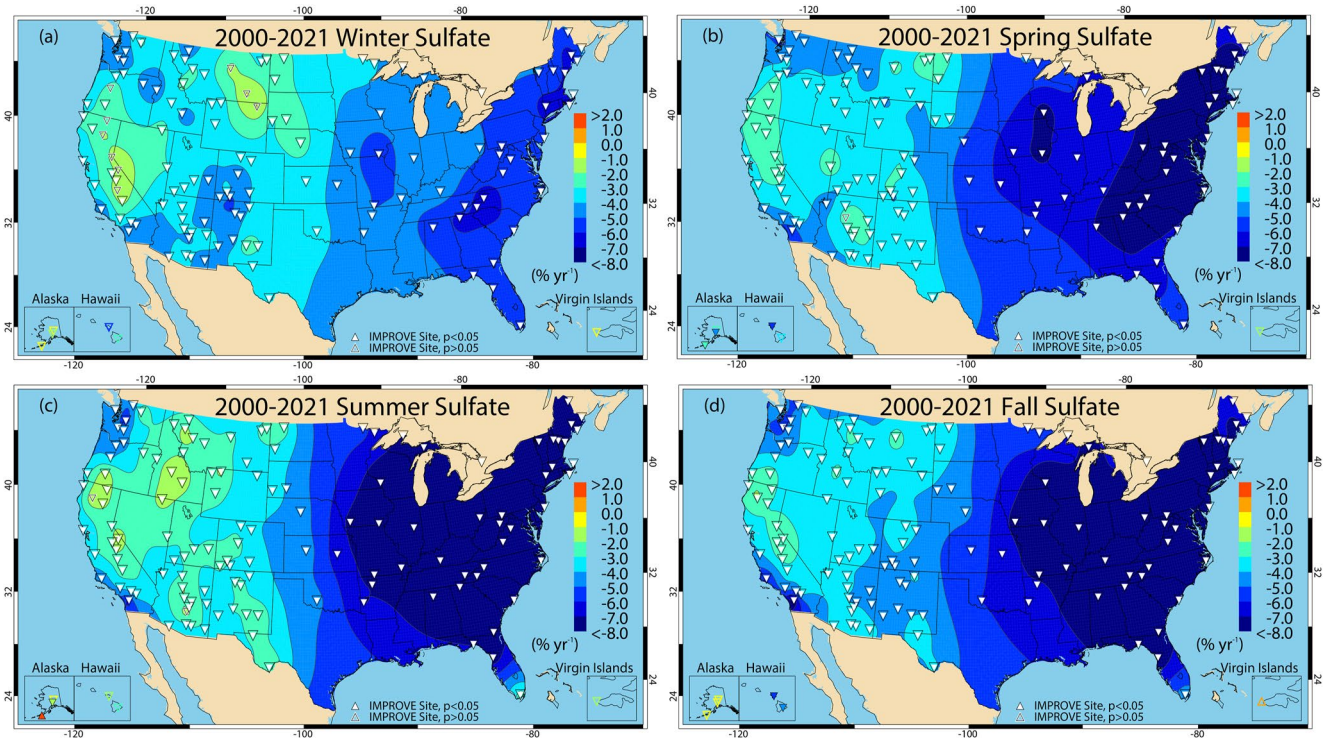

Figure 5. Seasonal mean sulfate ion concentration trends (% yr^{-1}) from 2000 to 2021 for (a) winter (DJF) (b) spring (MAM) (c) summer (JJA), and (d) fall (SON). Filled triangles correspond to statistically significant trends ($p \leq 0.05$).

concentrations are shown in the Supplemental Information (Figures S2–S6 in Supporting Information S1) and demonstrate the linear decrease in FM concentrations.

4.2. Sulfate

Seasonal mean sulfate ion concentrations decreased significantly across the United States during all seasons (Figure 5). The strongest reductions (−3 to −14% yr^{-1}) occurred at sites in the eastern United States, especially around Appalachia where SO_2 emissions have strongly decreased (Feng et al., 2020; Hand et al., 2020; Kharol et al., 2017; Krotkov et al., 2016). This reduction in sulfate has led to widespread improvements in visibility (Hand et al., 2020) and reductions in sulfate deposition (Benish et al., 2022; Sickles & Shadwick, 2015) and reductions have been reported in both rural and urban environments in the East due to the regional influence of sulfate (Blanchard et al., 2013; Hand, Schichtel, et al., 2012). Less progress has occurred for sites in the West, where emissions and concentrations are historically lower than at sites in the East (e.g., Hand, Schichtel, et al., 2012, 2020), and natural and international sources have larger relative contributions. Therefore, the reductions of regulated emissions have had less of an impact on already-low sulfate concentrations. Most trends in the West ranged from −2% yr^{-1} to −5% yr^{-1} during all seasons. The highest number of insignificant trends occurred during winter (Figure 5a) such as the group of sites in Montana and Wyoming, and California and Oregon. Stronger reductions at sites in the southwestern United States occurred during winter and fall relative to spring and summer (compare Figures 5a and 5d to Figures 5b and 5c, respectively). Concentrations at sites in southern California decreased more strongly than at sites in central California during all seasons, with the strongest reductions in southern California at the Agua Tibia (AGTI1) site (−5% yr^{-1} to −7% yr^{-1} depending on season). The greatest reductions in seasonal mean sulfate concentrations ranged from −14.5% yr^{-1} ($p < 0.001$) at Frostburg Reservoir, Maryland (FRRE1) in summer and at Cohutta, Georgia (COHU1) in fall (−14.5% yr^{-1}, $p < 0.001$). These are the same sites with the strongest reductions in FM. Concentrations significantly increased (1.3% yr^{-1}, $p = 0.027$) during summer at Simeon, Alaska (SIME1).

The spatial gradients and seasonal distribution in sulfate ion trends are summarized in the regional mean trends presented in Figure 6. The largest reductions in seasonal mean sulfate ion concentrations occurred for sites in

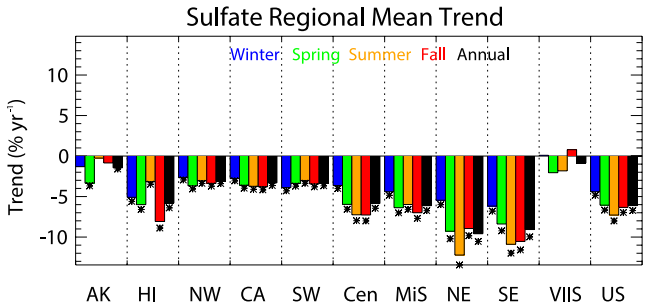

Figure 6. Regional, seasonal mean sulfate ion trends (% yr^{-1}) from 2002 to 2021 for major U.S. regions for winter, spring, summer, fall, and annual means. Regions are arranged from west to east United States (AK = Alaska, HI = Hawaii, NW = Northwest, CA = California, SW = Southwest, Cen = Central, MiS = Midsouth, NE = Northeast, SE = Southeast, VIIS = Virgin Islands, and US = all sites). Statistically significant trends ($p \leq 0.05$) are denoted with "*".

the Northeast region (−10.5% yr^{-1}, $p < 0.001$ in summer), followed by the Southeast region (−10.9% yr^{-1}, $p < 0.001$, in summer). These trends were similar to FM regional trends shown in Figure 4. For the Northeast and Southeast regions, the largest decrease in sulfate ion concentrations occurred during summer, while in the Midsouth region the decrease in fall was slightly larger. In all eastern regions the lowest decreases occurred during winter. This difference in seasonal mean trends has led to a decrease in the seasonality of sulfate ion concentrations (Chan et al., 2018), and may be due to the availability of oxidants (Paulot et al., 2017; Shah et al., 2018). In regions in the western United States, the rate of decrease was ∼−3% yr^{-1}, roughly half of that in the eastern regions. The differences in seasonal mean trends were also smaller, indicating that sulfate ion concentrations decreased by similar proportions across seasons. Summer trends in the Hawaii region were also lower than other seasons. However, overall, across the eastern United States, sulfate ion concentrations have decreased at a higher rate during summer and fall. Seasonal mean trends in Alaska and the Virgin Islands regions were relatively flat and insignificant, with the exception of spring and annual mean trends in the Alaska region. The annual mean sulfate trend across the United States was −6.1% yr^{-1} ($p < 0.001$). Timelines of regional and seasonal mean sulfate concentrations are shown in Figures S7–S11 in Supporting Information S1.

4.3. Nitrate

Trends in seasonal mean nitrate ion concentrations are shown in Figure 7. For all seasons, strong reductions occurred in southern California, at sites like San Gorgonio (SAGO1), Agua Tibia (AGTI1), and Joshua Tree (JOSH1), where statistically significant trends ranged from −8% yr^{-1} to −11% yr^{-1}, depending on season. The southern California area experienced significant reductions in NO_x emissions (Russell et al., 2012; Yu et al., 2021). Nitrate decreased at

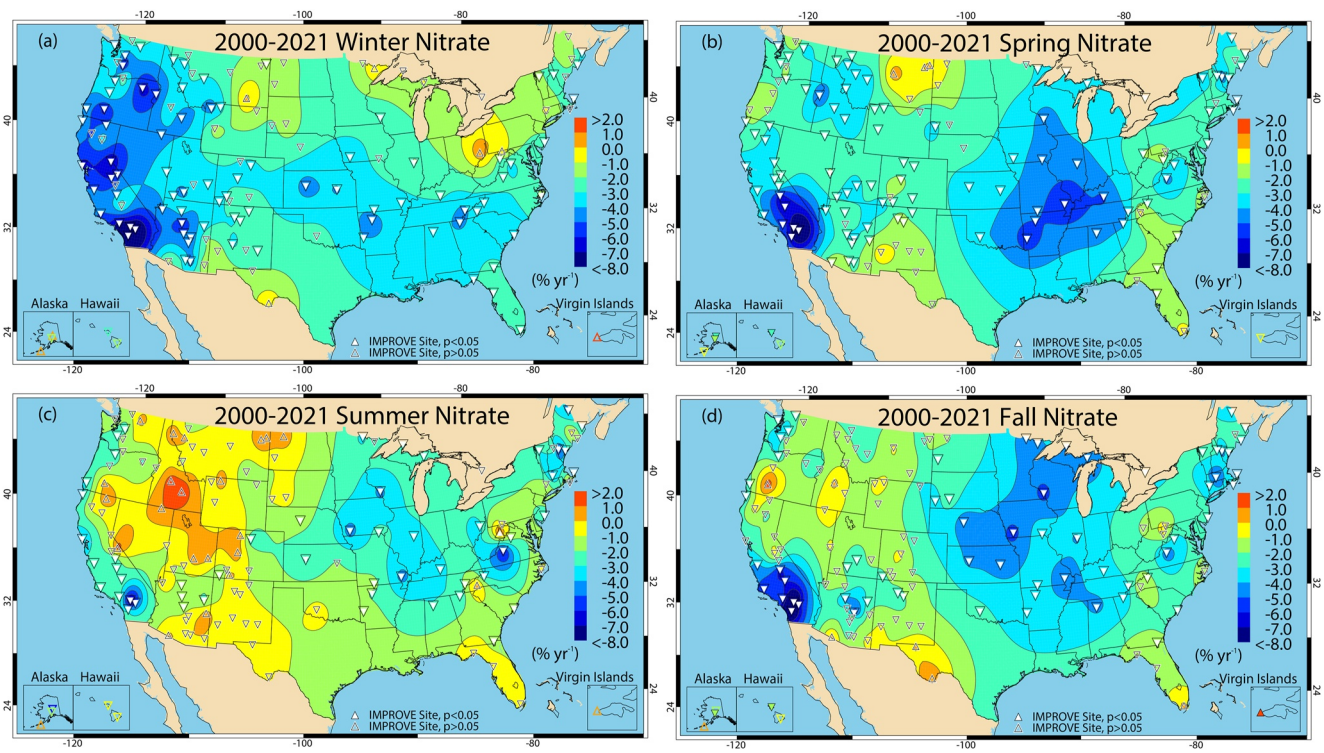

Figure 7. Seasonal mean nitrate ion concentration trends (% yr^{-1}) from 2000 to 2021 for (a) winter (DJF) (b) spring (MAM) (c) summer (JJA), and (d) fall (SON). Filled triangles correspond to statistically significant trends ($p \leq 0.05$).

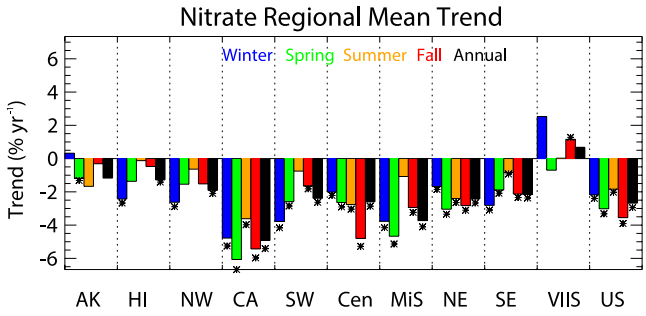

Figure 8. Regional, seasonal mean nitrate ion trends (% yr^{-1}) from 2002 to 2021 for major U.S. regions for winter, spring, summer, fall, and annual means. Regions are arranged from west to east (AK = Alaska, HI = Hawaii, NW = Northwest, CA = California, SW = Southwest, Cen = Central, MiS = Midsouth, NE = Northeast, SE = Southeast, VIIS = Virgin Islands, and US = all sites). Statistically significant trends ($p \leq 0.05$) are denoted with "*".

sites across the western United States and in the Midsouth and central United States, with the strongest reductions (−4% yr^{-1} to −5% yr^{-1}) in spring and fall (Figures 7b and 7d, respectively). Insignificant trends occurred at sites across the West during summer (Figure 7c); however, concentrations at many of these sites during summer tend to be lower than during cool months with conditions that favor particulate nitrate formation, and the annual mean concentrations shown in Figure 1b were relatively low. At sites in the Northern Great Plains, insignificant trends occurred at some sites during all seasons, likely due to the influence of oil and gas development in the region, offsetting reductions in other emission sectors (Evanoski-Cole et al., 2017; Gebhart et al., 2018; Hand, Gebhart, et al., 2012; Prenni et al., 2016). Seasonal mean trends ranged from −11.0% yr^{-1} ($p < 0.001$) during spring in Joshua Tree, California (JOSH1) and −11.9% yr^{-1} ($p < 0.001$) in San Gorgonio, California (SAGO1) in fall to 1.7% yr^{-1} ($p = 0.016$) in Dolly Sods, West Virginia (DOSO1) in summer and 1.6% yr^{-1} ($p = 0.021$) in the Virgin Islands (VIIS1) in fall.

Comparisons of regional and seasonal mean nitrate trends are shown in Figure 8. The strongest reductions in regional mean nitrate concentrations occurred in the California region, especially in spring (−6.1% yr^{-1}, $p < 0.001$) and fall (−5.4% yr^{-1}, $p < 0.006$); the lowest trends occurred during summer (−3.6% yr^{-1}, $p < 0.002$). A similar seasonal pattern in trends occurred in the Northwest and Southwest regions, with strong winter trends and insignificant summer trends. Other regions had different seasonal variability in trends. Most regions experienced the strongest reductions in winter or spring, with the exception of the Northeast region (similar reductions for all seasons), and the Central region. The Central region had the highest nitrate reductions in fall (−4.8% yr^{-1}, $p < 0.001$) with the lowest trends in winter (−2.0% yr^{-1}, $p = 0.044$). The OCONUS regions had mostly insignificant trends, with the exception of negative winter and annual mean trends in the Hawaii region, and positive fall mean trends in the Virgin Islands region (1.2% yr^{-1}, $p = 0.048$). The range in regional, seasonal mean trends that occurred across the United States indicated potentially different sources and atmospheric processes controlling nitrate concentrations across these regions. The total U.S. annual mean trend in nitrate was −2.7% yr^{-1} ($p < 0.001$), roughly half of the annual mean U.S. sulfate trend, perhaps in part due to other sources of unregulated NO_x and other nitrogen species such as ammonia (Li et al., 2016). Figures S12–S16 in Supporting Information S1 provide timelines of regional, seasonal mean nitrate concentrations.

4.4. Organic Carbon

Seasonal mean trends in OC had much greater spatial variability than sulfate and nitrate trends (Figure 9). Relatively strong reductions in OC have occurred at sites in the southeastern United States during all seasons (−2% yr^{-1} to −4% yr^{-1}) due to reductions in anthropogenic emissions (e.g., Blanchard et al., 2016; Malm et al., 2017; Ridley et al., 2018). OC also decreased at sites in the West but only during winter (Figure 9a) and spring (Figure 9b) (−3% yr^{-1} to −4% yr^{-1}). Insignificant winter trends, some positive, occurred at sites in the Central Valley of California and northern California, Oregon, Montana, Utah, Arizona, and the central United States. The spatial patterns in trends at sites in the West during summer and fall were very different than other seasons. With the exception of sites in southern California and Arizona, many of the sites across the West had insignificant positive trends. These trends indicate sources that regionally influence OC, such as biomass smoke emissions. As McClure and Jaffe (2018) reported, biomass smoke has influenced the highest $PM_{2.5}$ concentrations at sites across the Northwest. In fact, the similarities in spatial patterns between OC and FM trends in summer and fall (recall Figures 3c and 3d, respectively) suggest trends in OC are affecting seasonal and annual mean FM trends, especially since OC is a large fraction of the fine mass budget at sites in the West, as shown for several western regions in Figure 2. The statistically significant OC trends in summer and fall ranged from −5.4% yr^{-1} ($p < 0.001$) in Everglades, Florida (EVER1) to −0.9% yr^{-1} ($p = 0.009$) in Casco Bay, Maine (CABA1). In winter and spring, statistically significant trends ranged from −6.5% yr^{-1} ($p = 0.002$) in White River, Colorado (WHRI1) to −1.1% yr^{-1} ($p = 0.046$) in Ike's Backbone, Arizona (IKBA1).

Regional, seasonal mean OC trends are shown in Figure 10. Statistically significant trends occurred during all seasons in the Northeast and Southeast regions, around −2% yr^{-1} to −3% yr^{-1}. The strongest reductions in these regions occurred in winter. Trends in the Central U.S. region were lower than regions in the East (−1% yr^{-1} to −2% yr^{-1}) and statistically significant in winter and spring, but insignificant in summer and fall. Seasonal mean

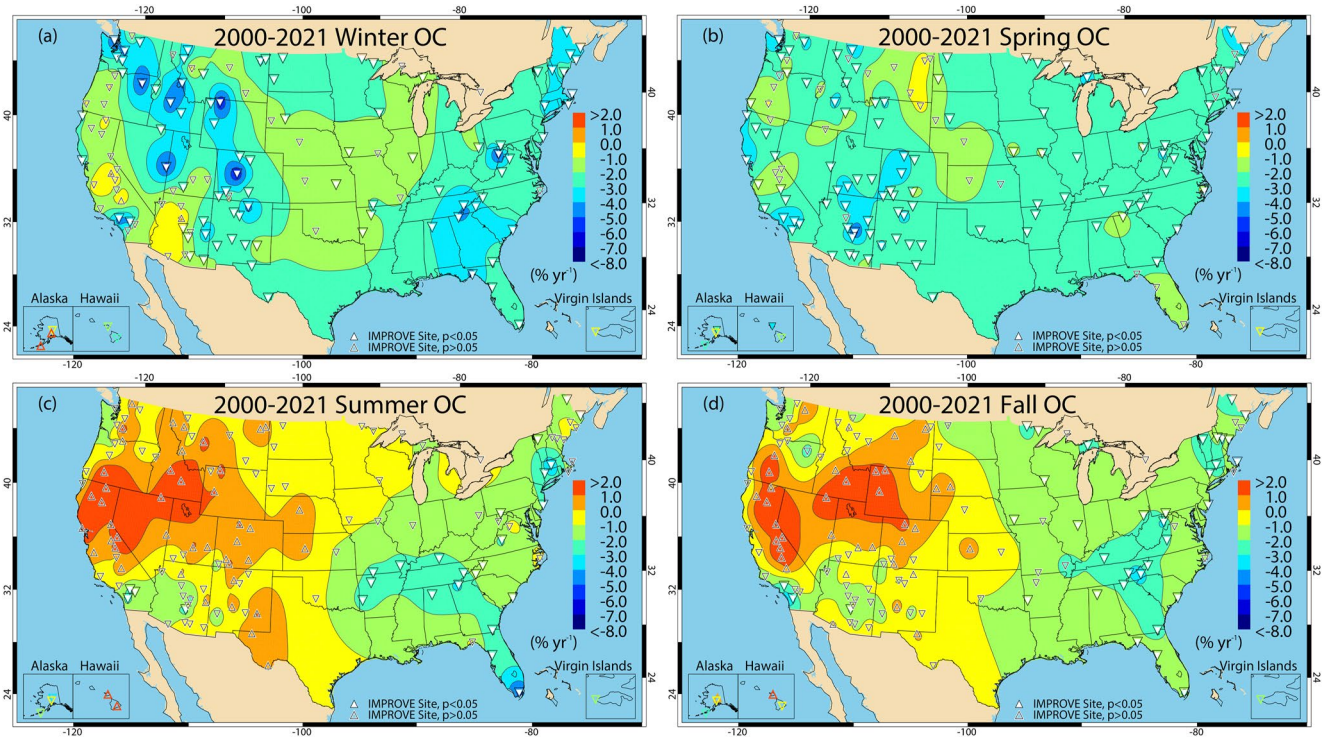

Figure 9. Seasonal mean organic carbon (OC) trends (% yr^{-1}) from 2000 to 2021 for (a) winter (DJF) (b) spring (MAM) (c) summer (JJA), and (d) fall (SON). Filled triangles correspond to statistically significant trends ($p \leq 0.05$).

trends at western regions were more variable than in the East. Regional mean winter and spring trends were negative and statistically significant in the Northwest and Southwest regions, and OC declined strongly in these seasons (−2% yr^{-1} to −3% yr^{-1}), similar to winter trends in eastern regions. However, western regional mean trends in summer and fall were insignificant and flat, especially in the Northwest and California regions. These patterns reflect the site-specific trends in Figure 9 and demonstrate the importance of seasonal sources, such as biomass burning emissions, on OC concentrations across the West. Similar regional and seasonal mean patterns were observed for FM (Figure 4). The annual mean OC trend for the United States was insignificant (−0.9% yr^{-1}, $p = 0.330$); OC was the only species with an insignificant annual mean U.S. trend. Timelines of these concentrations are found in Figures S17–S21 in Supporting Information S1.

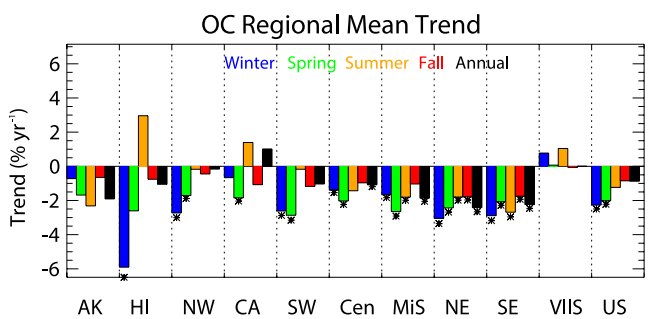

Figure 10. Regional, seasonal mean organic carbon (OC) trends (% yr^{-1}) from 2002 to 2021 for major U.S. regions for winter, spring, summer, fall, and annual means. Regions are arranged from west to east (AK = Alaska, HI = Hawaii, NW = Northwest, CA = California, SW = Southwest, Cen = Central, MiS = Midsouth, NE = Northeast, SE = Southeast, VIIS = Virgin Islands, and US = all sites). Statistically significant trends ($p \leq 0.05$) are denoted with "*".

4.5. Elemental Carbon

The spatial patterns in seasonal mean EC trends were somewhat similar to OC trends (Figure 11), especially with strong reductions at sites in the western United States in winter and spring (Figures 11a and 11b, respectively). Similarities in OC and EC trends reflect impacts from common combustion sources, such as biomass smoke in the West. Trends during winter and spring ranged from −8.8% yr^{-1} ($p < 0.001$) at San Gabriel, California (SAGA1) to −1.4% yr^{-1} ($p < 0.001$) at Medicine Lake, Montana (MELA1). Insignificant trends at sites in northern Montana and North Dakota are likely influenced by oil and gas development (Gebhart et al., 2018). At sites in the East, EC decreased significantly across the region during all seasons, but especially in summer (Figure 11c). However, in the West, trends in EC in summer and fall (Figures 11c and 11d, respectively) were mostly statistically insignificant, similar to insignificant trends for OC, and were likely also influenced by biomass smoke. Trends during summer and fall ranged from −7.1% yr^{-1} ($p < 0.001$) at San Gorgonio, California (SAGO1) to 2.5% yr^{-1} ($p = 0.045$) at

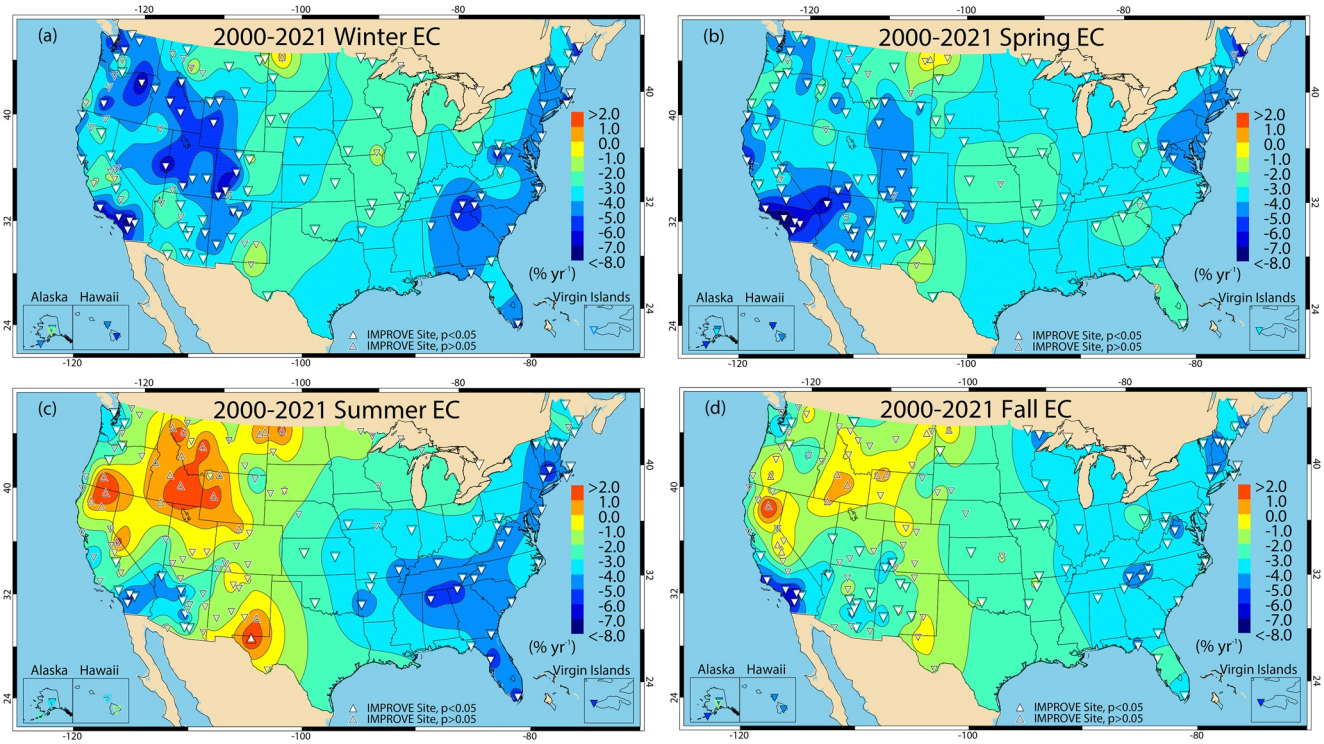

Figure 11. Seasonal mean elemental carbon (EC) trends (% yr^{-1}) from 2000 to 2021 for (a) winter (DJF) (b) spring (MAM) (c) summer (JJA), and (d) fall (SON). Filled triangles correspond to statistically significant trends ($p \leq 0.05$).

Guadalupe Mountains, Texas (GUMO1). Guadalupe Mountains is near areas with oil and gas development, and these emissions have influenced air quality at nearby sites (Benedict et al., 2020; Naimie et al., 2022).

Regional, seasonal mean trends are summarized in Figure 12 and corresponding timelines are shown in Figures S22–S26 in Supporting Information S1. Negative, and mostly statistically significant trends occurred for all regions and seasons, with the exception of summer and fall trends in western regions, such as the Northwest, and California regions. In these regions, negative and statistically significant winter and spring trends (−4% yr^{-1} to −5% yr^{-1}) contrasted the insignificant and flat trends in EC during summer and fall, likely reflecting the influence of biomass burning emissions on EC concentrations. This pattern shifts for the Central region, with similar magnitudes in statistically significant trends during all seasons (∼−2% yr^{-1}). In eastern regions, stronger reductions were observed during summer (∼−4% yr^{-1}), contrasting summer trends in western regions. Summer mean EC trends in Hawaii were flat and insignificant, but EC decreased strongly in other seasons. The difference in seasonal and regional trends across the United States implies different sources that influenced EC depending on region and season, especially with respect to East versus West, and summer versus winter. The success of regulatory activity that led to reductions of EC in the East (Blanchard et al., 2016; Hidy et al., 2014; Murphy et al., 2011) contrasts the impacts of biomass smoke emissions that hindered similar progress in summer in regions of the West.

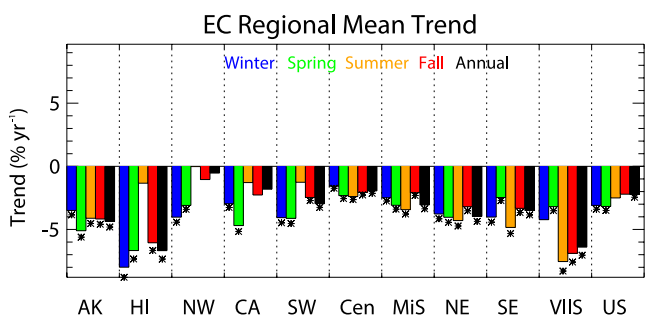

Figure 12. Regional, seasonal mean elemental carbon (EC) trends (% yr^{-1}) from 2002 to 2021 for major U.S. regions for winter, spring, summer, fall, and annual means. Regions are arranged from west to east (AK = Alaska, HI = Hawaii, NW = Northwest, CA = California, SW = Southwest, Cen = Central, MiS = Midsouth, NE = Northeast, SE = Southeast, VIIS = Virgin Islands, and US = all sites). Statistically significant trends ($p \leq 0.05$) are denoted with "*".

4.6. Fine Dust

Seasonal mean trends in FD demonstrated a high degree of spatial variability (Figure 13) and had the fewest number of sites with statistically significant trends of any species. The strongest reductions in FD occurred during winter at sites in the eastern United States (Figure 13a), around −5% yr^{-1} to −6% yr^{-1}. Spatial patterns of trends in winter mean FD had negative trends at sites in the Northwest and Northern Great Plains, but insignificant trends

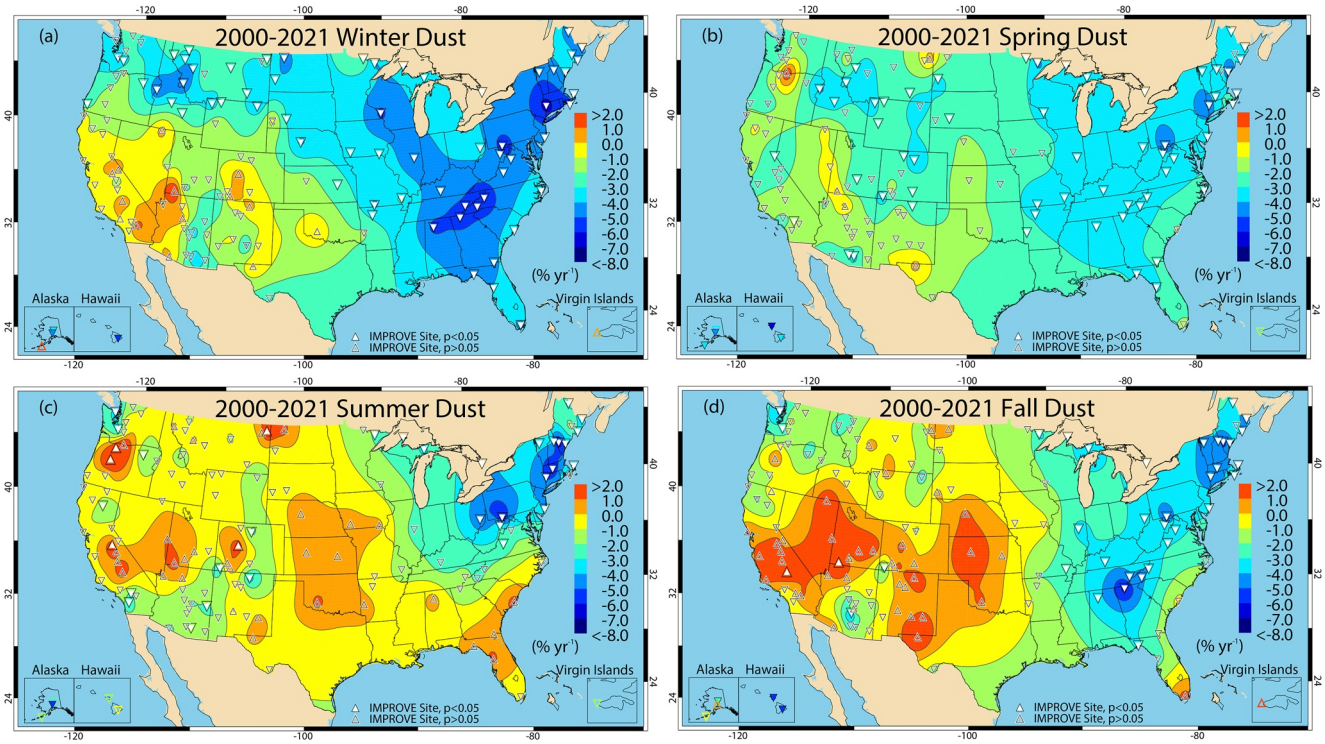

Figure 13. Seasonal mean fine dust (FD) trends (% yr^{-1}) from 2000 to 2021 for (a) winter (DJF) (b) spring (MAM) (c) summer (JJA), and (d) fall (SON). Filled triangles correspond to statistically significant trends ($p \leq 0.05$).

at sites across California and the Southwest. Trends in spring (Figure 13b) were generally less negative than during winter across the United States, with some exceptions, including sites in Arizona, Washington, Montana, and North Dakota. Winter and spring CONUS trends ranged from −6.7% yr^{-1} ($p < 0.001$) in Mohawk Mountain, Connecticut (MOMO1) to −1.5% yr^{-1} ($p = 0.028$) in Martha's Vineyard, Massachusetts (MAVI1). Most of the trends in summer and fall were insignificant, especially at sites in the central and western United States (Figures 13c and 13d, respectively), where several local and regional dust sources exist (Ginoux et al., 2012). Insignificant trends at sites in the Northern Great Plains were likely associated with fugitive dust emissions associated with oil and gas development (Bar-Ilan et al., 2011; Gebhart et al., 2018), as these sites also had insignificant trends in nitrate, OC, and EC. Statistically significant positive trends occurred in both summer and fall. In summer, seven sites had positive trends, with the highest (>2% yr^{-1}) at Mount Hood, Oregon (2.3% yr^{-1}, $p = 0.040$, MOHO1), Medicine Lake, Montana (2.9% yr^{-1}, $p = 0.001$, MELA1), and Three Sisters, Oregon (4.2% yr^{-1}, $p = 0.017$, THSI1). During fall, statistically significant positive trends occurred at two sites, including Dome Lands, California (2.7% yr^{-1}, $p = 0.025$, DOME1) and Zion Canyon, Utah (4.7% yr^{-1}, $p = 0.021$, ZICA1). Summer trends at sites in the Southeast were insignificant.

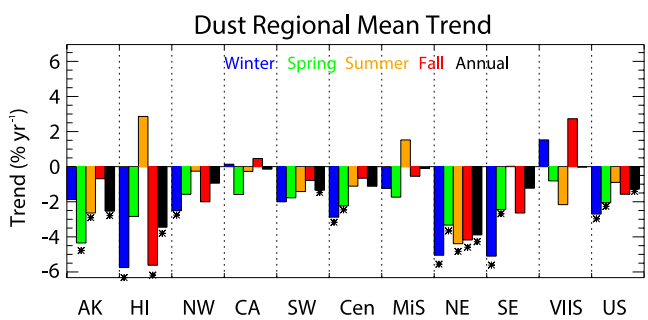

Figure 14. Regional, seasonal mean fine dust (FD) trends (% yr^{-1}) from 2002 to 2021 for major U.S. regions for winter, spring, summer, fall, and annual means. Regions are arranged from west to east (AK = Alaska, HI = Hawaii, NW = Northwest, CA = California, SW = Southwest, Cen = Central, MiS = Midsouth, NE = Northeast, SE = Southeast, VIIS = Virgin Islands, and US = all sites). Statistically significant trends ($p \leq 0.05$) are denoted with "*".

Regional, seasonal mean FD trends were mostly insignificant and generally less negative compared to other species (Figure 14). Only the Northeast region had statistically significant negative trends during all seasons, with the strongest reduction in winter (−5.1% yr^{-1}, $p < 0.001$). The Southeast region had statistically significant reductions in FD during winter and spring and a flat trend during summer, when transport of North African dust regularly influences sites in the region. Similarly, the Midsouth region had insignificant but positive trends during summer. In the Central region, only winter and spring had statistically significant negative trends (~−2% yr^{-1}); summer, fall, and annual mean trends were insignificant. Across the West, regions had insignificant though negative or flat trends. The California

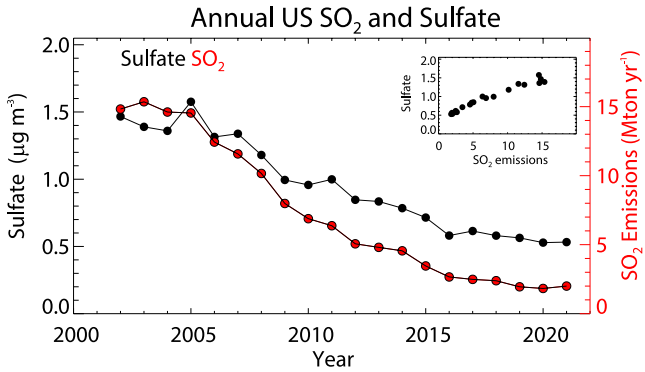

Figure 15. Total U.S. annual mean sulfate ion concentration (left axis, μg m^{-3}) and National Emission Inventory total annual SO_2 emissions (right axis, Mton yr^{-1}). The insert is a scatter plot of annual mean sulfate concentrations and SO_2 emissions (same units).

region had insignificant but positive trends during fall, and the summer trend in the Northwest region was flat. Many of the seasonal mean trends in the OCONUS regions were insignificant, except for spring, summer and annual mean trends in the Alaska region, and winter, fall, and annual mean trends in the Hawaii region. The annual mean FD trend across the United States was −1.3% yr^{-1} ($p = 0.009$). FD has not experienced the levels of reduction as sulfate and nitrate, in part because dust has more natural sources and therefore its trends are less influenced by changes in anthropogenic emissions. FD timelines corresponding to the trends shown in Figure 14 can be found in Figures S27–S31 in Supporting Information S1.

4.7. Emissions

Comparisons of emissions and concentrations are constrained by the spatial irregularity of both monitors and emissions, and therefore interpretations are limited due to both spatial and temporal disparity. However, the impacts of these irregularities are reduced due to long-range transport and mixing across regional scales. Overall, these comparisons are informative as to the response of concentrations to changes in emissions. Sulfate concentrations have decreased in response to reductions in SO_2 emissions due to regulations. A timeline of the NEI total annual SO_2 emissions and U.S. annual mean sulfate concentrations is shown in Figure 15, with an inset of a scatter plot of SO_2 emissions and sulfate concentrations. Total annual U.S. SO_2 emissions have declined by 87% between 2002 and 2021. SO_2 emissions and sulfate concentrations were highly correlated ($r = 0.98$, $p < 0.001$), and a linear Theil regression slope suggested a reduction of 0.070 ± 0.003 μg m^{-3} of sulfate per Mton yr^{-1} reduction of SO_2 emissions and an intercept of 0.48 ± 0.03 μg m^{-3} (± one standard error), reflecting additional SO_2 emission sources not included in the inventory. These values were similar to those reported by Hand et al. (2020) (slope of 0.072 ± 0.005 μg m^{-3} per Mton yr^{-1} and intercept of 0.51 ± 0.05 μg m^{-3}) for data from 2002 through 2018 at rural IMPROVE sites, as expected given the similarities in time periods.

As shown in Figure 16, NO_x emissions have dropped by 70% from 2002 to 2021. NO_x emissions and annual mean nitrate concentrations were highly correlated ($r = 0.93$, $p < 0.001$) and a linear Theil regression resulted in a slope of 0.010 ± 0.001 μg m^{-3} per Mton yr^{-1} NO_x emissions, suggesting that on average the response of nitrate concentrations to NO_x emission reductions was not as strong as for sulfate. One possible explanation is that particulate nitrate formation was ammonia-limited in many rural areas of the United States. With the decrease in sulfate, more ammonia is available to neutralize nitric acid; however, declines in NO_x emissions make this less true today (e.g., Feng et al., 2020; Gu et al., 2021; Nenes et al., 2020).

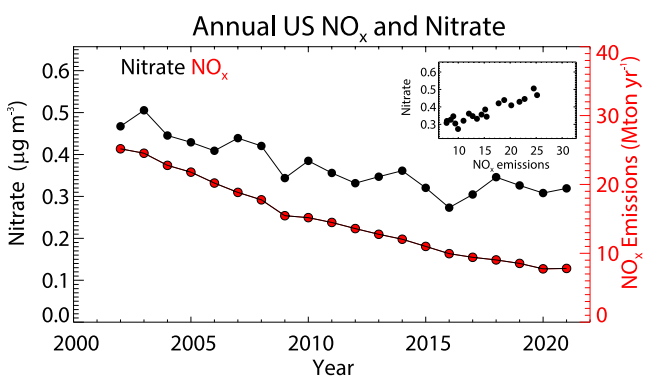

Figure 16. Total U.S. annual mean nitrate ion concentration (left axis, μg m^{-3}) and National Emission Inventory total annual NO_x emissions (right axis, Mton yr^{-1}). The insert is a scatter plot of annual mean nitrate concentrations and NO_x emissions (same units).

An intercept of 0.21 ± 0.02 μg m^{-3} also suggested missing sources of NO_x in the emission inventory, including oil and gas and agricultural emissions (Dix et al., 2020; Gebhart et al., 2018; Pozzer et al., 2017; Thompson et al., 2017). These results are similar to previous estimates from earlier years (2002–2018) from Hand et al. (2020) who reported a slope of 0.014 ± 0.002 μg m^{-3} per Mton yr^{-1} and intercept of 0.16 ± 0.03 μg m^{-3}. Nitrate contributes significantly to FM in the Central U.S. region (Figure 1), and agricultural sources of nitrate are important in this region (Pitchford et al., 2009; Pozzer et al., 2017).

Given the impacts on OC and EC concentrations from biomass burning emissions, a comparison of total U.S. wildland burn area and total U.S. annual mean OC concentrations is shown in Figure 17a, with a correlation coefficient of $r = 0.47$ ($p = 0.08$). Burn area includes contributions from the entire U.S. and not all OC is due to fire emissions, so it is only a rough comparison. Comparing annual mean OC concentrations from only the Northwest region to total annual burn area increased the correlation to $r = 0.52$ ($p = 0.016$). After 2015, total annual OC concentrations follow burn area more closely, corresponding to high fire years in 2017–2018 and 2020–2021. Total annual NEI VOC emissions are shown with annual mean OC concentrations in

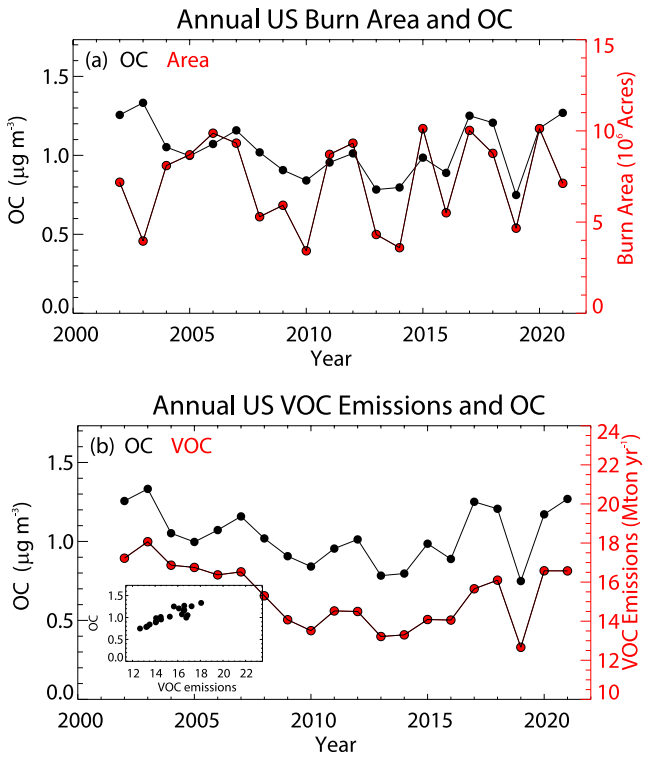

Figure 17. (a) Total U.S. annual mean organic carbon (OC) concentration (left axis, μg m^{-3}) and total U.S. wildland fire burn area (right axis, 10^6 acres) (b) total U.S. annual mean OC concentration (left axis, μg m^{-3}) and total annual U.S. National Emission Inventory volatile organic carbon (VOC) emissions (right axis, Mton yr^{-1}).

Figure 17b, with an inset of a scatter plot of VOC emissions and OC concentrations. The correlation coefficient was $r = 0.89$ ($p < 0.001$), much higher than for OC and burn area. However, the fraction of VOC emissions due to wildfires has increased over the last two decades, from 8% in 2002 to 28% in 2021 (see Figure S32 in Supporting Information S1). Malm et al. (2017) also showed a high likelihood that much of the reduction in OC in the East in summer and fall can be attributed to reduced sulfate concentrations and sulfate catalyzed OC formation.

Total annual mean EC concentrations and total U.S. annual burn area is shown in Figure 18a, and black carbon (BC) emissions from the NEI are shown in Figure 18b. The correlation of EC with NEI BC emissions was higher ($r = 0.77$; $p < 0.001$) than with burn area (0.37; $p = 0.190$). The NEI BC emissions include wildfire, and the fraction of BC from wildfire emissions increased from 4% to 40% from 2002 to 2021 (see Figure S32 in Supporting Information S1). For both NEI OC and BC emissions, wildfire has an increased impact over the past two decades.

In the Southwest region, OC and sulfate contributed similar fractions to FM on an annual basis (Figure 1e), but FD was the major contributor. FD concentrations in the United States are highest in the Southwest (Figure 1e) and trends in the region have been linked to meteorological conditions such as drought (Achakulwisut et al., 2019) and large-scale climate variability (Hand et al., 2016; Pu & Ginoux, 2018). For example, the negative phase of the PDO has been associated with drought in the Southwest (e.g., Weiss et al., 2009). Hand et al. (2016) identified an inverse relationship between regional, March monthly mean FD in the Southwest and the March PDO index from 1995 through 2014 ($r = -0.65$). Later years were included here to compare Southwest regional, spring mean FD and March PDO indices from 2002 through 2021 (Figure 19). The y-axis for the PDO index is reversed as negative PDO indices tend to correspond to higher FD concentrations. A correlation coefficient of $r = -0.46$ ($p = 0.032$) suggested that the PDO has influence on the seasonal FD concentrations in the region.

5. Summary

Reductions in FM have occurred at nearly all remote regions and nearly all seasons across the United States. These reductions were strongest for regions in the East (especially in summer) and were driven by negative trends in sulfate ion concentrations, although negative trends in nitrate and OC concentrations in the eastern regions have also contributed (e.g., Blanchard et al., 2016; Hidy et al., 2014; Malm et al., 2017; Ridley et al., 2018). Overall, annual mean FM trends decreased at a rate of -1.8% yr^{-1} ($p < 0.001$). For individual species, sulfate had the strongest reduction in total annual mean U.S. concentrations (-6.1% yr^{-1}, $p < 0.001$), followed by nitrate (-2.7% yr^{-1}, $p < 0.001$), and EC (-2.2% yr^{-1}, $p = 0.027$). The lowest reductions corresponded to FD (-1.3% yr^{-1}, $p = 0.009$) and OC (-0.9% yr^{-1}, $p = 0.330$).

FM has declined at a weaker rate in regions in the West relative to eastern regions, especially during summer and fall due to the major contributions from OC. While OC decreased significantly across regions in the East during all seasons, likely due to successful regulatory activity, OC trends at regions in the West were flat and insignificant during the fire seasons of summer and fall. This influence will likely hinder future progress in FM reductions, especially in the West. The lessons learned regarding successful regulatory activity that have resulted in reduced FM and speciated composition could be applied to managing other unregulated anthropogenic sources, such as oil and gas and agricultural emissions. As regulated precursors continue to decline, other sources will grow in importance. These sources include unregulated anthropogenic sources, as well as natural sources such as wildfire and dust, which are also predicted to increase with climate change.

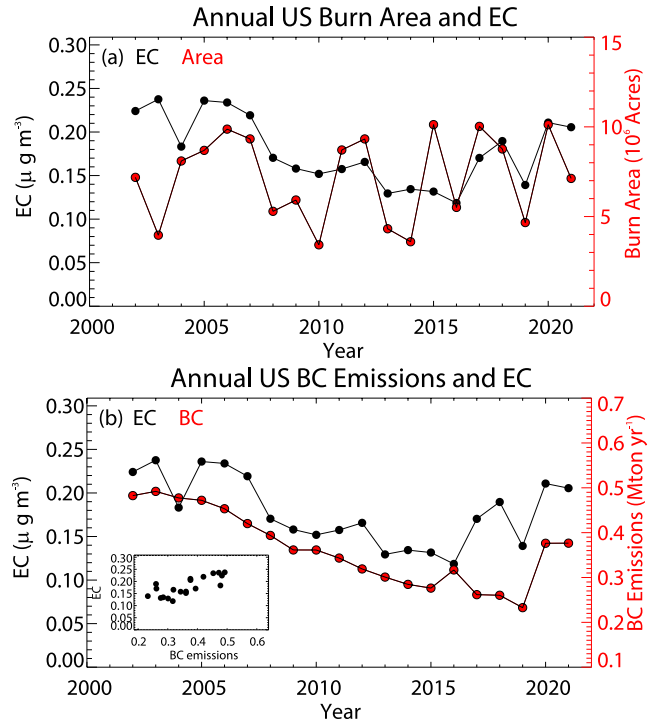

Figure 18. (a) Total U.S. annual mean elemental carbon (EC) concentration (left axis, μg m^{-3}) and total U.S. wildland fire burn area (right axis, 10^6 acres) (b) total U.S. annual mean EC concentration (left axis, μg m^{-3}) and total annual U.S. National Emission Inventory black carbon (BC) emissions (right axis, Mton yr^{-1}).

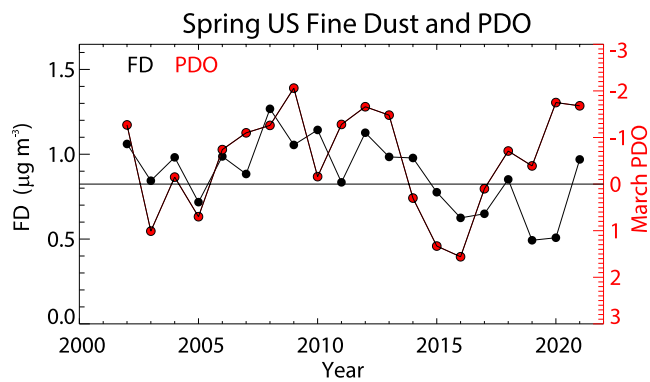

Figure 19. Southwest spring (MAM) mean fine dust (FD) concentrations (left-axis, μg m^{-3}) and the March Pacific Decadal Oscillation index (right axis, reversed).

Conflict of Interest

The authors declare no conflicts of interest relevant to this study.

Data Availability Statement

These datasets are publicly available, as follows:

IMPROVE: Federal Land Manager Environmental Database (http://views.cira.colostate.edu/fed/)

EPA National Emission Inventory (https://www.epa.gov/air-emissions-inventories/air-pollutant-emissions-trends-data)

National Interagency Fire Center (https://www.nifc.gov/fire-information/statistics/wildfires)

Pacific Decadal Oscillation Index from the National Centers for Environmental Information (NCEI) (https://www.ncei.noaa.gov/access/monitoring/pdo/).

Acknowledgments
This work was funded by the National Park Service Air Resources Division under task agreement number P21AC11375-03 under Cooperative Agreement P17AC00971 and views presented herein are those of the authors and should not be interpreted as necessarily representing the National Park Service. IMPROVE is a collaborative association of state, tribal, and federal agencies, and international partners. The U.S. Environmental Protection Agency (EPA) is the primary funding source, with contracting and research support from the National Park Service. The Air Quality Group at the University of California, Davis, is the central analytical laboratory, with ion analysis provided by the Research Triangle Institute and carbon analysis provided by the Desert Research Institute.

References

Achakulwisut, P., Anenberg, S. C., Neumann, J. E., Penn, S. L., Weiss, N., Crimmins, A., et al. (2019). Effects of increasing aridity on ambient dust and public health in the US Southwest under climate change. *GeoHealth*, *3*(5), 127–144. https://doi.org/10.1029/2019GH000187

Aldhaif, A. M., Lopez, D. H., Dadashazar, H., & Sorooshian, A. (2020). Sources, frequency, and chemical nature of dust events impacting the United States East Coast. *Atmospheric Environment*, *231*, 12. https://doi.org/10.1016/j.atmosenv.2020.117456

Attwood, A., Washenfelder, R., Brock, C., Hu, W., Baumann, K., Campuzano-Jost, P., et al. (2014). Trends in sulfate and organic aerosol mass in the Southeast US: Impact on aerosol optical depth and radiative forcing. *Geophysical Research Letters*, *41*(21), 7701–7709. https://doi.org/10.1002/2014GL061669

Bar-Ilan, A., Grant, J., Parikh, R., Morris, R., Heath, G., Diakov, V., et al. (2011). Moving towards improved basin-level oil and gas inventories and reconciliation with measurements: Final report to EPA. 41. Retrieved from https://www.wrapair2.org/pdf/2011-07_P3%20Study%20Report%20(Final%20July-2011).pdf

Beachley, G., Phuchalski, M., Rogers, C., & Lear, G. (2016). A summary of long-term trends in sulfur and nitrogen deposition in the United States 1990–2013. *JSM Environmental Science & Ecology*, *4*(2), 1030.

Benedict, K. B., Prenni, A. J., El-Sayed, M. M., Hecobian, A., Zhou, Y., Gebhart, K. A., et al. (2020). Volatile organic compounds and ozone at four national parks in the southwestern United States. *Atmospheric Environment*, *239*, 117783. https://doi.org/10.1016/j.atmosenv.2020.117783

Benish, S. E., Bash, J. O., Foley, K. M., Wyat Appel, K., Hogrefe, C., Gilliam, R., & Pouliot, G. (2022). Long-term regional trends of nitrogen and sulfur deposition in the United States from 2002 to 2017. *Atmospheric Chemistry and Physics*, *22*(19), 12749–12767. https://doi.org/10.5194/acp-22-12749-2022

Blanchard, C., Hidy, G., Shaw, S., Baumann, K., & Edgerton, E. (2016). Effects of emission reductions on organic aerosol in the southeastern United States. *Atmospheric Chemistry and Physics*, *16*(1), 215–238. https://doi.org/10.5194/acp-16-215-2016

Blanchard, C., Hidy, G., Tanenbaum, S., Edgerton, E., & Hartsell, B. (2013). The Southeastern Aerosol Research and Characterization (SEARCH) study: Temporal trends in gas and PM concentrations and composition, 1999–2010. *Journal of the Air & Waste Management Association*, *63*(3), 247–259. https://doi.org/10.1080/10962247.2012.748523

Bond, T. C., Doherty, S. J., Fahey, D. W., Forster, P. M., Berntsen, T., DeAngelo, B. J., et al. (2013). Bounding the role of black carbon in the climate system: A scientific assessment. *Journal of Geophysical Research: Atmospheres*, *118*(11), 5380–5552. https://doi.org/10.1002/jgrd.50171

Bozlaker, A., Prospero, J. M., Price, J., & Chellam, S. (2019). Identifying and quantifying the impacts of advected North African dust on the concentration and composition of airborne fine particulate matter in Houston and Galveston, Texas. *Journal of Geophysical Research: Atmospheres*, *124*(22), 12282–12300. https://doi.org/10.1029/2019JD030792

Chan, E. A. W., Gantt, B., & McDow, S. (2018). The reduction of summer sulfate and switch from summertime to wintertime PM2.5 concentration maxima in the United States. *Atmospheric Environment*, *175*, 25–32. https://doi.org/10.1016/j.atmosenv.2017.11.055

Chen, Y., Shen, H., & Russell, A. G. (2019). Current and future responses of aerosol ph and composition in the US to declining SO2 emissions and increasing NH3 emissions. *Environmental Science & Technology*, *53*(16), 9646–9655. https://doi.org/10.1021/acs.est.9b02005

Chow, J., Watson, J., Chen, L.-W., Rice, J., & Frank, N. (2010). Quantification of PM 2.5 organic carbon sampling artifacts in US networks. *Atmospheric Chemistry and Physics*, *10*(12), 5223–5239. https://doi.org/10.5194/acp-10-5223-2010

Chow, J. C., Watson, J. G., Chen, L.-W. A., Chang, M. O., Robinson, N. F., Trimble, D., & Kohl, S. (2007). The IMPROVE_A temperature protocol for thermal/optical carbon analysis: Maintaining consistency with a long-term database. *Journal of the Air & Waste Management Association*, *57*(9), 1014–1023. https://doi.org/10.3155/1047-3289.57.9.1014

Chow, J. C., Watson, J. G., Lowenthal, D. H., & Magliano, K. L. (2005). Loss of PM2.5 nitrate from filter samples in central California. *Journal of the Air & Waste Management Association*, *55*(8), 1158–1168. https://doi.org/10.1080/10473289.2005.10464704

Creamean, J. M., Spackman, J. R., Davis, S. M., & White, A. B. (2014). Climatology of long-range transported Asian dust along the West Coast of the United States. *Journal of Geophysical Research: Atmospheres*, *119*(21), 12171–112185. https://doi.org/10.1002/2014JD021694

Debell, L. J. (2006). Data validation historical report NO3. Retrieved from http://vista.cira.colostate.edu/improve/wp-content/uploads/2022/09/044_Historical_QA_Report_Nitrate.pdf

Dix, B., de Bruin, J., Roosenbrand, E., Vlemmix, T., Francoeur, C., Gorchov-Negron, A., et al. (2020). Nitrogen oxide emissions from US oil and gas production: Recent trends and source attribution. *Geophysical Research Letters*, *47*(1), 9. https://doi.org/10.1029/2019gl085866

Du, E., de Vries, W., Galloway, J. N., Hu, X., & Fang, J. (2014). Changes in wet nitrogen deposition in the United States between 1985 and 2012. *Environmental Research Letters*, *9*, 095004. https://doi.org/10.1088/1748-9362/9/9/095004

Ellis, R., Jacob, D. J., Sulprizio, M. P., Zhang, L., Holmes, C., Schichtel, B., et al. (2013). Present and future nitrogen deposition to national parks in the United States: Critical load exceedances. *Atmospheric Chemistry and Physics*, *13*(17), 9083–9095. https://doi.org/10.5194/acp-13-9038-2013

Evanoski-Cole, A., Gebhart, K., Sive, B., Zhou, Y., Capps, S., Day, D., et al. (2017). Composition and sources of winter haze in the Bakken oil and gas extraction region. *Atmospheric Environment*, *156*, 77–87. https://doi.org/10.1016/j.atmosenv.2017.02.019

Feng, J., Chan, E., & Vet, R. (2020). Air quality in the eastern United States and eastern Canada for 1990–2015: 25 years of change in response to emission reductions of SO2 and NOx in the region. *Atmospheric Chemistry and Physics*, *20*(5), 3107–3134. https://doi.org/10.5194/acp-20-3107-2020

Field, J. P., Belnap, J., Breshears, D. D., Neff, J. C., Okin, G. S., Whicker, J. J., et al. (2010). The ecology of dust. *Frontiers in Ecology and the Environment*, *8*(8), 423–430. https://doi.org/10.1890/090050

Frank, N. H. (2006). Retained nitrate, hydrated sulfates, and carbonaceous mass in federal reference method fine particulate matter for six eastern US cities. *Journal of the Air & Waste Management Association*, *56*(4), 500–511. https://doi.org/10.1080/10473289.2006.10464517

Gan, C.-M., Pleim, J., Mathur, R., Hogrefe, C., Long, C. N., Xing, J., et al. (2015). Assessment of long-term WRF-CMAQ simulations for understanding direct aerosol effects on radiation "brightening" in the United States. *Atmospheric Chemistry and Physics*, *15*(21), 12193–12209. https://doi.org/10.5194/acp-15-12193-2015

Gebhart, K. A., Day, D. E., Prenni, A. J., Schichtel, B. A., Hand, J. L., & Evanoski-Cole, A. R. (2018). Visibility impacts at Class I areas near the Bakken oil and gas development. *Journal of the Air & Waste Management Association*, *68*(5), 477–493. https://doi.org/10.1080/10962247.2018.1429334

Ginoux, P., Prospero, J. M., Gill, T. E., Hsu, N. C., & Zhao, M. (2012). Global-scale attribution of anthropogenic and natural dust sources and their emission rates based on MODIS Deep Blue aerosol products. *Reviews of Geophyics*, *50*(3), RG3005. https://doi.org/10.1029/2012RG000388

Gu, B., Zhang, L., Van Dingenen, R., Vieno, M., Van Grinsven, H. J. M., Zhang, X., et al. (2021). Abating ammonia is more cost effective than nitrogen oxides for mitigating $PM_{2.5}$ air pollution. *Science*, *374*(6568), 758–762. https://doi.org/10.1126/science.abf8623

Hand, J. L., Copeland, S. A., Chow, J., Dillner, A. M., Hyslop, N. P., Prenni, A. J., et al. (2023). *IMPROVE (Interagency monitoring of Protected Visual Environments): Spatial and seasonal patterns and temporal variability of haze and its constituents in the United States, IMPROVE Report VI*. Cooperative Institute for Research in the Atmosphere, Colorado State University. https://doi.org/10.25675/10217/237177

Hand, J. L., Gebhart, K. A., Schichtel, B. A., & Malm, W. C. (2012). Increasing trends in wintertime particulate sulfate and nitrate ion concentrations in the Great Plains of the United States (2000–2010). *Atmospheric Environment*, *55*, 107–110. https://doi.org/10.1016/j.atmosenv.2012.03.050

Hand, J. L., Gill, T., & Schichtel, B. (2017). Spatial and seasonal variability in fine mineral dust and coarse aerosol mass at remote sites across the United States. *Journal of Geophysical Research: Atmospheres*, *122*(5), 3080–3097. https://doi.org/10.1002/2016JD026290

Hand, J. L., Prenni, A. J., Copeland, S., Schichtel, B. A., & Malm, W. C. (2020). Thirty years of the Clean Air Act Amendments: Impacts on haze in remote regions of the United States (1990–2018). *Atmospheric Environment*, *243*, 117865. https://doi.org/10.1016/j.atmosenv.2020.117865

Hand, J. L., Prenni, A. J., Schichtel, B. A., Malm, W. C., & Chow, J. C. (2019). Trends in remote PM2.5 residual mass across the United States: Implications for aerosol mass reconstruction in the IMPROVE network. *Atmospheric Environment*, *203*, 141–152. https://doi.org/10.1016/j.atmosenv.2019.01.049

Hand, J. L., Schichtel, B. A., Malm, W. C., Copeland, S., Molenar, J. V., Frank, N. H., & Pitchford, M. (2014). Widespread reductions in haze across the United States from the early 1990s through 2011. *Atmospheric Environment*, *94*, 671–679. https://doi.org/10.1016/j.atmosenv.2014.05.062

Hand, J. L., Schichtel, B. A., Malm, W. C., & Pitchford, M. L. (2012). Particulate sulfate ion concentration and SO2 emission trends in the United States from the early 1990s through 2010. *Atmospheric Chemistry and Physics*, *12*(21), 10353–10365. https://doi.org/10.5194/acp-12-10353-2012

Hand, J. L., White, W., Gebhart, K., Hyslop, N., Gill, T., & Schichtel, B. (2016). Earlier onset of the spring fine dust season in the southwestern United States. *Geophysical Research Letters*, *43*(8), 4001–4009. https://doi.org/10.1002/2016GL068519

Heald, C., Collett, J. L., Lee, T., Benedict, K. B., Schwandner, F. M., Li, Y., et al. (2012). Atmospheric ammonia and particulate inorganic nitrogen over the United States. *Atmospheric Chemistry and Physics*, *12*(21), 10295–10312. https://doi.org/10.5194/acp-12-10295-2012

Hering, S., & Cass, G. (1999). The magnitude of bias in the measurement of PM25 arising from volatilization of particulate nitrate from Teflon filters. *Journal of the Air & Waste Management Association*, *49*(6), 725–733. https://doi.org/10.1080/10473289.1999.10463843

Hidy, G., Blanchard, C., Baumann, K., Edgerton, E., Tanenbaum, S., Shaw, S., et al. (2014). Chemical climatology of the southeastern United States, 1999–2013. *Atmospheric Chemistry and Physics*, *14*(21), 11893–11914. https://doi.org/10.5194/acp-14-11893-2014

Hu, C., Griffis, T. J., Baker, J. M., Wood, J. D., Millet, D. B., Yu, Z., & Lee, X. (2020). Modeling the sources and transport processes during extreme ammonia episodes in the US Corn Belt. *Journal of Geophysical Research: Atmospheres*, *125*(2), e2019JD031207. https://doi.org/10.1029/2019JD031207

Husar, R. B., Holloway, J. M., Patterson, D. E., & Wilson, E. (1981). Spatial and temporal pattern of eastern US haziness: A summary. *Atmospheric Environment*, *10*(1), 1919–1928. https://doi.org/10.1016/0004-6981(81)90226-2

Husar, R. B., Tratt, D., Schichtel, B. A., Falke, S., Li, F., Jaffe, D., et al. (2001). Asian dust events of April 1998. *Journal of Geophysical Research*, *106*(D16), 18317–18330. https://doi.org/10.1029/2000JD900788

Hyslop, N. P., Trzepla, K., & White, W. H. (2015). Assessing the suitability of historical PM2. 5 element measurements for trend analysis. *Environmental Science & Technology*, *49*(15), 9247–9255. https://doi.org/10.1021/acs.est.5b01572

Isaaks, E. H., & Mohan Srivastava, R. (1989). *An introduction to applied geostatistics*. Oxford University Press.

Kharol, S. K., McLinden, C. A., Sioris, C. E., Shephard, M. W., Fioletov, V., van Donkelaar, A., et al. (2017). OMI satellite observations of decadal changes in ground-level sulfur dioxide over North America. *Atmospheric Chemistry and Physics*, *17*(9), 5921–5929. https://doi.org/10.5194/acp-17-5921-2017

Kim, D., Chin, M., Cruz, C. A., Tong, D., & Yu, H. (2021). Spring dust in western North America and its interannual variability—Understanding the role of local and transported dust. *Journal of Geophysical Research: Atmospheres*, *126*(22), e2021JD035383. https://doi.org/10.1029/2021JD035383

Kim, P. S., Jacob, D. J., Fisher, J. A., Travis, K., Yu, K., Zhu, L., et al. (2015). Sources, seasonality, and trends of southeast US aerosol: An integrated analysis of surface, aircraft, and satellite observations with the GEOS-Chem chemical transport model. *Atmospheric Chemistry and Physics*, *15*(18), 10411–10433. https://doi.org/10.5194/acp-15-10411-2015

Krotkov, N. A., McLinden, C. A., Li, C., Lamsal, L. N., Celarier, E. A., Marchenko, S. V., et al. (2016). Aura OMI observations of regional SO2 and NO2 pollution changes from 2005 to 2015. *Atmospheric Chemistry and Physics*, *16*(7), 4605–4629. https://doi.org/10.5194/acp-16-4605-2016

Lambert, A., Hallar, A. G., Garcia, M., Strong, C., Andrews, E., & Hand, J. L. (2020). Dust impacts of rapid agricultural expansion on the Great Plains. *Geophysical Research Letters*, *47*(20), e2020GL090347. https://doi.org/10.1029/2020GL090347

Lawal, A. S., Guan, X., Liu, C., Henneman, L. R., Vasilakos, P., Bhogineni, V., et al. (2018). Linked response of aerosol acidity and ammonia to SO2 and NOx emissions reductions in the United States. *Environmental Science & Technology*, *52*(17), 9861–9873. https://doi.org/10.1021/acs.est.8b00711

Lehmann, C. M., & Gay, D. A. (2011). Monitoring long-term trends of acidic wet deposition in US precipitation: Results from the National Atmospheric Deposition Program. *PowerPlant Chemistry*, *13*(7), 378–385.

Leibensperger, E. M., Mickley, L. J., Jacob, D. J., Chen, W.-T., Seinfeld, J. H., Nenes, A., et al. (2012). Climatic effects of 1950-2050 changes in US anthropogenic aerosols – Part 1: Aerosol trends and radiative forcing. *Atmospheric Chemistry and Physics*, *12*(7), 3333–3348. https://doi.org/10.5194/acp-12-3333-2012

Li, Y., Schichtel, B. A., Walker, J. T., Schwede, D. B., Chen, X., Lehmann, C. M. B., et al. (2016). Increasing importance of deposition of reduced nitrogen in the United States. *Proceedings of the National Academy of Sciences*, *113*(21), 5874–6579. https://doi.org/10.1073/pnas.1525736113

Lowenthal, D., & Kumar, N. (2006). Light scattering from sea-salt aerosols at Interagency monitoring of Protected Visual Environments (IMPROVE) sites. *Journal of the Air & Waste Management Association*, *56*(5), 636–642. https://doi.org/10.1080/10473289.2006.10464478

Lowenthal, D., Zielinska, B., Samburova, V., Collins, D., Taylor, N., & Kumar, N. (2015). Evaluation of assumptions for estimating chemical light extinction at US national parks. *Journal of the Air & Waste Management Association*, *65*(3), 249–260. https://doi.org/10.1080/10962247.2014.986307

Malm, W., Schichtel, B., Hand, J., & Prenni, A. (2020). Implications of organic mass to carbon ratios increasing over time in the rural United States. *Journal of Geophysical Research: Atmospheres*, *125*(5), e2019JD031480. https://doi.org/10.1029/2019JD031480

Malm, W. C., Schichtel, B. A., Ames, R. B., & Gebhart, K. A. (2002). A 10-year spatial and temporal trend of sulfate across the United States. *Journal of Geophysical Research*, *107*(D22), 4627. https://doi.org/10.1029/2002JD002107

Malm, W. C., Schichtel, B. A., Hand, J. L., & Collett, J. L., Jr. (2017). Concurrent temporal and spatial trends in sulfate and organic mass concentrations measured in the IMPROVE monitoring program. *Journal of Geophysical Research: Atmospheres*, *122*(19), 10462–10476. https://doi.org/10.1002/2017JD026865

Malm, W. C., Sisler, J. F., Huffman, D., Eldred, R. A., & Cahill, T. A. (1994). Spatial and seasonal trends in particle concentration and optical extinction in the United States. *Journal of Geophysical Research*, *99*(D1), 1347–1370. https://doi.org/10.1029/93JD02916

McClure, C. D., & Jaffe, D. A. (2018). US particulate matter air quality improves except in wildfire-prone areas. *Proceedings of the National Academy of Sciences*, *115*(31), 7901–7906. https://doi.org/10.1073/pnas.1804353115

McDade, C. (2004). Summary of IMPROVE nitrate measurements. http://vista.cira.colostate.edu/improve/Publications/GrayLit/025_IMPROVEnitrate/Nitrate%20Summary_1004.pdf

McDade, C. (2007). Diminished wintertime nitrate concentrations in late 1990s, *IMPROVE Data Advisory Document* #da0002. http://vista.cira.colostate.edu/improve/Data/QA_QC/Advisory/da0002/da0002_WinterNO3.pdf

Murphy, D. M., Chow, J. C., Leibensperger, E. M., Malm, W. C., Pitchford, M., Schichtel, B. A., et al. (2011). Decreases in elemental carbon and fine particle mass in the United States. *Atmospheric Chemistry and Physics*, *11*(10), 4679–4686. https://doi.org/10.5194/acp-11-4679-2011

Murphy, D. M., Froyd, K. D., Bian, H., Brock, C. A., Dibb, J. E., DiGangi, J. P., et al. (2019). The distribution of sea-salt aerosol in the global troposphere. *Atmospheric Chemistry and Physics*, *19*(6), 4093–4104. https://doi.org/10.5194/acp-19-4093-2019

Naimie, L. E., Sullivan, A. P., Benedict, K. B., Prenni, A. J., Sive, B. C., Schichtel, B. A., et al. (2022). PM2.5 in Carlsbad Caverns National Park: Composition, sources, and visibility impacts. *Journal of the Air & Waste Management Association*, *72*(11), 1201–1218. https://doi.org/10.1080/10962247.2022.2081634

Nenes, A., Pandis, S. N., Weber, R. J., & Russell, A. (2020). Aerosol pH and liquid water content determine when particulate matter is sensitive to ammonia and nitrate availability. *Atmospheric Chemistry and Physics*, *20*(5), 3249–3258. https://doi.org/10.5195/acp-20-3249-2020

Nopmongcol, U., Beardsley, R., Kumar, N., Knipping, E., & Yarwood, G. (2019). Changes in United States deposition of nitrogen and sulfur compounds over five decades from 1970 to 2020. *Atmospheric Environment*, *209*, 144–151. https://doi.org/10.1016/j.atmosenv.2019.04.018

Park, R. J., Jacob, D. J., Field, B. D., Yantosca, R. M., & Chin, M. (2004). Natural and transboundary pollution influences on sulfate-nitrate-ammonium aerosols in the United States: Implications for policy. *Journal of Geophysical Research*, *109*(D15), D15204. https://doi.org/10.1029/2003JD004473

Park, R. J., Jacob, D. J., Kumar, N., & Yantosca, R. M. (2006). Regional visibility statistics in the United States: Natural and transboundary pollution influences, and implications for the Regional Haze Rule. *Atmospheric Environment*, *40*(28), 5405–5423. https://doi.org/10.1016/j.atmosenv.2006.04.059

Paulot, F., Fan, S., & Horowitz, L. (2017). Contrasting seasonal responses of sulfate aerosols to declining SO2 emissions in the Eastern US: Implications for the efficacy of SO2 emission controls. *Geophysical Research Letters*, *44*(1), 455–464. https://doi.org/10.1002/2016GL070695

Perry, K. D., Cahill, T. A., Eldred, R. A., Dutcher, D. D., & Gill, T. E. (1997). Long-range transport of North African dust to the eastern United States. *Journal of Geophysical Research*, *102*(D10), 11225–11238. https://doi.org/10.1029/97JD00260

Petzold, A., Ogren, J. A., Fiebig, M., Laj, P., Li, S. M., Baltensperger, U., et al. (2013). Recommendations for reporting "black carbon" measurements. *Atmospheric Chemistry and Physics*, *13*(16), 8365–8379. https://doi.org/10.5194/acp-13-8365-2013

Pitchford, M., Poirot, R., Schichtel, B. A., & Malm, W. C. (2009). Characterization of the winter midwestern particulate nitrate bulge. *Journal of the Air & Waste Management Association*, *59*(9), 1061–1069. https://doi.org/10.3155/1047-3289.59.9.1061

Pozzer, A., Tsimpidi, A. P., Karydis, V. A., de Meij, A., & Lelieveld, J. (2017). Impact of agricultural emission reductions on fine-particulate matter and public health. *Atmospheric Chemistry and Physics*, *17*(20), 12813–12826. https://doi.org/10.5194/acp-17-12813-2017

Prenni, A., Day, D., Evanoski-Cole, A., Sive, B., Hecobian, A., Zhou, Y., et al. (2016). Oil and gas impacts on air quality in federal lands in the Bakken region: An overview of the Bakken Air Quality Study and first results. *Atmospheric Chemistry and Physics*, *16*(3), 1401–1416. https://doi.org/10.5194/acp-16-1401-2016

Prenni, A. J., Benedict, K. B., Day, D. E., Sive, B. C., Zhou, Y., Naimie, L., et al. (2022). Wintertime haze and ozone at Dinosaur National Monument. *Journal of the Air & Waste Management Association*, *72*(9), 951–968. https://doi.org/10.1080/10962247.2022.2048922

Prospero, J. M., Delany, A. C., Delany, A. C., & Carlson, T. N. (2021). The discovery of African dust transport to the Western Hemisphere and the Saharan air layer: A history. *Bulletin of the American Meteorological Society*, *102*(6), E1239–E1260. https://doi.org/10.1175/BAMS-D-19-0309.1

Prospero, J. M., Ginoux, P., Torres, O., Nicholson, S. E., & Gill, T. E. (2002). Environmental characterization of global sources of atmospheric soil dust identified with the Nimbus 7 Total Ozone Mapping Spectrometer (TOMS) absorbing aerosol product. *Reviews of Geophysics*, *40*(1), 2-1–2-31. https://doi.org/10.1029/2000RG000095

Pu, B., & Ginoux, P. (2018). Climatic factors contributing to long-term variations in surface fine dust concentration in the United States. *Atmospheric Chemistry and Physics*, *18*(6), 4201–4215. https://doi.org/10.5194/acp-18-4201-2018

Ridley, D. A., Heald, C. L., Ridley, K. J., & Kroll, J. H. (2018). Causes and consequences of decreasing atmospheric organic aerosol in the United States. *Proceedings of the National. Academies of Science*, *115*(2), 290–295. https://doi.org/10.1073/pnas.1700387115

Rivera, N. I. R., Gill, T. E., Gebhart, K. A., Hand, J. L., Bleiweiss, M. P., & Fitzgerald, R. M. (2009). Wind modeling of Chihuahuan Desert dust outbreaks. *Atmospheric Environment*, *43*(2), 347–354. https://doi.org/10.1016/j.atmosenv.2008.09.069

Russell, A., Valin, L., & Cohen, R. (2012). Trends in OMI NO2 observations over the United States: Effects of emission control technology and the economic recession. *Atmospheric Chemistry and Physics*, *12*(24), 12197–12209. https://doi.org/10.5194/acp-12-12197-2012

Samset, B. H., Sand, M., Smith, C. J., Bauer, S. E., Forster, P. M., Fuglestvedt, J. S., et al. (2018). Climate impacts from a removal of anthropogenic aerosol emissions. *Geophysical Research Letters*, *45*(2), 1020–1029. https://doi.org/10.1002/2017gl076079

Schichtel, B. A., Hand, J. L., Barna, M. G., Gebhart, K. A., Copeland, S., Vimont, J., & Malm, W. C. (2017). Origin and fine particulate carbon in the rural United States. *Environmental Science and Technology*, *51*(17), 9846–9855. https://doi.org/10.1021/acs.est.7b00645

Schichtel, B. A., Malm, W. C., Beaver, M., Copeland, S., Hand, J. L., Prenni, A. J., et al. (2021). The future of carbonaceous aerosol measurement in the IMPROVE monitoring program. http://vista.cira.colostate.edu/improve/wp-content/uploads/2021/10/041_CarbonReport_Final.pdf

Schichtel, B. A., Pitchford, M. L., & White, W. H. (2011). Comments on "Impact of California's Air Pollution Laws on Black Carbon and their Implications for Direct Radiative Forcing" by R. Bahadur et al. *Atmospheric Environment*, *45*(24), 4116–4118. https://doi.org/10.1016/j.atmosenv.2011.04.042

Seinfeld, J. H., Bretherton, C., Carslaw, K. S., Coe, H., DeMott, P. J., Dunlea, E. J., et al. (2016). Improving our fundamental understanding of the role of aerosol-cloud interactions in the climate system. *Proceedings of the National Academies of Science*, *113*(21), 5781–5790. https://doi.org/10.1073/pnas.1514043113

Shah, V., Jaeglé, L., Thornton, J. A., Lopez-Hilfiker, F. D., Lee, B. H., Schroder, J. C., et al. (2018). Chemical feedbacks weaken the wintertime response of particulate sulfate and nitrate to emissions reductions over the eastern United States. *Proceedings of the National Academies of Science*, *115*(32), 8110–8115. https://doi.org/10.1073/pnas.1803295115

Shi, Q. R., Zheng, B., Zheng, Y., Tong, D., Liu, Y., Ma, H., et al. (2022). Co-benefits of CO2 emission reduction from China's clean air actions between 2013–2020. *Nature Communications*, *13*(1), 8. https://doi.org/10.1038/s41467-022-32656-8

Shiraiwa, M., Ueda, K., Pozzer, A., Lammel, G., Kampf, C. J., Fushimi, A., et al. (2017). Aerosol health effects from molecular to global scales. *Environmental Science & Technology*, *51*(23), 13545–13567. https://doi.org/10.1021/acs.est.7b04417

Sickles, J. E., & Shadwick, D. S. (2015). Air quality and atmospheric deposition in the eastern US: 20 years of change. *Atmospheric Chemistry and Physics*, *15*(1), 173–197. https://doi.org/10.5194/acp-15-173-2015

Silvern, R. F., Jacob, D. J., Kim, P. S., Marais, E. A., Turner, J. R., Campuzano-Jost, P., & Jimenez, J. L. (2017). Inconsistency of ammonium–sulfate aerosol ratios with thermodynamic models in the eastern US: A possible role of organic aerosol. *Atmospheric Chemistry and Physics*, *17*(8), 5107–5118. https://doi.org/10.5194/acp-17-5107-2017

Spada, N. J., Yatkin, S., Giacomo, J., Trzepla, K., & Hyslop, N. P. (2023). Evaluating IMPROVE PM2.5 element measurements. *Journal of the Air & Waste Management Association*, *73*(11), 843–852. https://doi.org/10.1080/10962247.2023.2262417

Theil, H. (1950). A rank-invariant method of linear and polynomial regression analysis. *Proceedings of the Koninklijke Nederlandse Akademie van Wetenschappen, A*(53), 386–392. https://doi.org/10.1007/978094-011-2546-8_20

Thompson, T. M., Shepherd, D., Stacy, A., Barna, M. G., & Schichtel, B. A. (2017). Modeling to evaluate contribution of oil and gas emissions to air pollution. *Journal of the Air & Waste Management Association*, *67*(4), 445–461. https://doi.org/10.1080/10962247.2016.1251508

Tong, D., Dan, M., Wang, T., & Lee, P. (2012). Long-term dust climatology in the western United States reconstructed from routine aerosol ground monitoring. *Atmospheric Chemistry and Physics*, *12*(11), 5189–5205. https://doi.org/10.5194/acp-12-5189-2012

Vitousek, P. M., Aber, J. D., Howarth, R. W., Likens, G. E., Matson, P. A., Schindler, D. W., et al. (1997). Human alteration of the global nitrogen cycle: Sources and consequences. *Ecological Applications*, *7*(3), 737–750. https://doi.org/10.1890/1051-0761(1997)007[0737:HAOTGN]2.0.CO;2

Warner, J., Dickerson, R., Wei, Z., Strow, L., Wang, Y., & Liang, Q. (2017). Increased atmospheric ammonia over the world's major agricultural areas detected from space. *Geophysical Research Letters*, *44*(6), 2875–2884. https://doi.org/10.1002/2016GL072305

Watson, J. G., Chow, J. C., Chen, L.-W. A., & Frank, N. H. (2009). Methods to assess carbonaceous aerosol sampling artifacts for IMPROVE and other long-term networks. *Journal of the Air & Waste Management Association*, *59*(8), 898–911. https://doi.org/10.3155/1047-3289.59.8.898

Weber, R. J., Guo, H., Russell, A. G., & Nenes, A. (2016). High aerosol acidity despite declining atmospheric sulfate concentrations over the past 15 years. *Nature Geoscience*, *9*(4), 282–285. https://doi.org/10.1038/NGEO2665

Weiss, J. L., Castro, C. L., & Overpeck, J. T. (2009). Distinguishing pronounced droughts in the southwestern United States: Seasonality and effects of warmer temperatures. *Journal of Climate*, *22*(22), 5918–5932. https://doi.org/10.1175/2009jcli2905.1

White, W. H. (2006). Elemental concentrations of Al above the MDL can go undetected, *IMPROVE Data Advisory Document* #da0010. http://vista.cira.colostate.edu/improve/Data/QA_QC/Advisory/da0010/da0010_Almdl.pdf

White, W. H. (2007). Shift in EC/OC split with 1 January 2005 TOR hardware upgrade, *IMPROVE Data Advisory Document* #da0016. http://vista.cira.colostate.edu/improve/Data/QA_QC/Advisory/da0016/da0016_TOR2005.pdf

White, W. H. (2008). Chemical markers for sea salt in IMPROVE aerosol data. *Atmospheric Environment*, *42*(2), 261–274. https://doi.org/10.1016/j.atmosenv.2007.09.040

White, W. H. (2016). Increased variation of humidity in the weighing laboratory, *IMPROVE Data Advisory Document* #da0035. http://vista.cira.colostate.edu/improve/Data/QA_QC/Advisory/da0035/da0035_IncreasedRH.pdf

Xing, J., Mathur, R., Pleim, J., Hogrefe, C., Gan, C.-M., Wong, D. C., et al. (2015). Observations and modeling of air quality trends over 1990-2010 across the Northern Hemisphere: China, the United States and Europe. *Atmospheric Chemistry and Physics*, *15*(5), 2723–2747. https://doi.org/10.5194/acp-15-2723-2015

Xu, L., Pye, H. O. T., He, J., Chen, Y., Murphy, B. N., & Ng, N. L. (2018). Experimental and model estimates of the contributions from biogenic monoterpenes and sesquiterpenes to secondary organic aerosol in the southeastern United States. *Atmospheric Chemistry and Physics*, *18*(17), 12613–12637. https://doi.org/10.5149/acp-18-12613-2018

Yu, K. A., McDonald, B. C., & Harley, R. A. (2021). Evaluation of nitrogen oxide emission inventories and trends for on-road gasoline and diesel vehicles. *Environmental Science & Technology*, *55*(10), 6655–6664. https://doi.org/10.1021/acs.est.1c00586

Zhang, X. (2019). Correction of chloride concentrations for filter blank levels, *IMPROVE Data Advisory Document* #da0039. http://vista.cira.colostate.edu/improve/Data/QA_QC/Advisory/da0039/da0039_ChlorideOverCorrection.pdf

Zhang, Y., Mathur, R., Bash, J. O., Hogrefe, C., Xing, J., & Roselle, S. J. (2018). Long-term trends in total inorganic nitrogen and sulfur deposition in the US from 1990 to 2010. *Atmospheric Chemistry and Physics*, *18*(12), 9091–9106. https://doi.org/10.5194/acp-18-9091-2018